Efficient Triplet Formation with a Covalently-Linked Bichromophore Comprising Weakly-Coupled TIPS-Pentacene Subunits: Accounting for the Energy Balance

Joshua K. G. Karlsson,[¶] Alparslan Atahan,[¶,†] Anthony Harriman,[¶,*] Nikolai V. Tkachenko,[§] Andrew D. Ward,[‡] Fabio A. Schaberle,[#] Carlos Serpa,[#] and Luis G. Arnaut[#]

[¶]Molecular Photonics Laboratory, School of Natural and Environmental Sciences, Bedson Building, Newcastle University, Newcastle upon Tyne, NE1 7RU, U.K.

[§]Faculty of Engineering and Natural Sciences, Tampere University, Koereakoulunkatu 7, FIN-33720 Tampere, Finland

[‡]Central Laser Facility, Research Complex at Harwell, STFC Rutherford Appleton Laboratory, Didcot, OX11 0FA, U.K.

[#]CQC, Department of Chemistry, University of Coimbra, 3004-535 Coimbra, Portugal

ABSTRACT: A covalently-linked bichromophore, comprising TIPS-pentacene terminals bridged by a fluorene spacer, generates a relatively high yield (i.e., 65 ± 5 %) of the spin-correlated, triplet biexciton upon illumination in toluene. Under the same conditions, the extent of fluorescence quenching exceeds 98% relative to the parent TIPS-pentacene and is insensitive to temperature. The biexciton, having overall singlet spin multiplicity, undergoes triplet-triplet annihilation, giving a minor crop of delayed fluorescence, in competition to spin decorrelation. These latter processes occur on the relatively slow timescale of ca. 100 ns, possibly reflecting the restricted level of electronic communication between the terminals. Decorrelation leads to formation of an isolated (i.e., independent) triplet pair, which is formed with an overall quantum efficiency of 44 ± 8 % and has a lifetime of almost 10 μs in de-aerated toluene. The triplet species exhibits phosphorescence at room temperature, both as a solid and in solution, allowing identification of the triplet excitation energy as 7,290 ± 200 cm^{-1}. This value is only slightly less than one-half of the corresponding singlet excitation energy and is in line with the appearance of delayed fluorescence. With the derived triplet energy, photoacoustic calorimetry (PAC) is used to refine the various quantum yields determined by optical spectroscopy. The PAC results indicate three separate enthalpy changes; a very fast step associated with intramolecular singlet exciton fission to form the correlated triplet biexciton, a fast step reflecting intramolecular triplet-triplet annihilation, and a slow step, not resolved by the transducer, due to relaxation of the independent triplet pair. At each stage, radiationless decay competes with triplet evolution. Both fluorescence quenching and triplet formation are enhanced in polar solvents at the expense of radiationless decay.

INTRODUCTION

Singlet exciton fission (SEF) is a spin-allowed process occurring with particular organic chromophores whereby a singlet-excited state generates two triplet excited states localized on neighboring molecules. The SEF mechanism has long been a curiosity in the field of molecular photophysics.[1-3] The subject received sporadic investigation over several decades until the realization that triplet state multiplication might be a potential route for enhancing the performance of certain types of organic solar cells.[4] This promising application has fuelled an exhaustive investigation into the mechanism[5,6] and optimization[7,8] of SEF with numerous different classes of organic chromophores. An intriguing, and perhaps unique, feature of SEF is that the corresponding reverse process, namely triplet-triplet annihilation to produce a crop of delayed fluorescence,[9] is also a strong candidate for advancing solar cell performance.[10,11] The early work in the SEF arena has been reviewed comprehensively by Smith and Michl[12,13] but many new aspects have been exposed in more recent studies. Perhaps the most important feature of the SEF process involves establishing a correct energy balance in terms of the relative excitation energies for excited-singlet and excited-triplet species. This is not as easy as it might appear since the SEF event gives rise to a triplet biexciton rather than the isolated triplet state. Indeed, spin decorrelation[14] and subsequent diffusion[15,16] of the triplet species are subjects of much current debate. Also under intense investigation are the possible roles of charge-transfer interactions[17,18] and vibrational coherence[19] in the SEF process. Detailed mechanistic studies are rendered difficult, however, by the fact that the degree of electronic coupling between proximal chromophores is strongly influenced by the molecular topology.[20-22] This situation arises because most SEF studies are carried out with condensed materials, such as single crystals or thin films.

At least in principle, many of the experimental challenges associated with the advanced spectroscopic study of solid-state samples can be overcome by the use of covalently-linked bichromophores or higher-order accretions.[23] This strategy, which is readily amenable to the systematic variation of molecular topology and mutual electronic coupling, was employed by Michl *et al*[24] in 2013 and applied to the study of weakly-coupled 1,3-diphenylisobenzofuran bichromophores. Despite the fact that the parent compound undergoes highly efficacious SEF in the solid state,[25] no triplet formation was evident for the bichromophores in nonpolar solvents. This was not the case with a small series of bis-pentacene derivatives reported by Guldi *et*

al[26] where triplet yields exceeding 100% were realized. Subsequently, a seemingly inexhaustible variety of molecular architectures has been reported[23] in an effort to obtain highly efficient triplet formation. Typical variations include modifications of the nature and number of chromophores,[27,28] the length[29] and electronic properties[30] of the connecting bridge, the singlet-triplet energy gap,[31-34] the mutual molecular orientation,[35] the nature of the surrounding medium[36] and the mode of excitation.[37] Competition between SEF and other photophysical processes, such as excimer formation[38] or light-induced charge transfer,[39] has been explored, as has the effect of SEF exergonicity.[40]

Progress in the generic field of intramolecular SEF (iSEF) has been reviewed recently by Johnson *et al*[23] with emphasis on what lessons have been learned and what remains to be clarified. An advantage of the covalently-linked chromophores relative to solid-state materials is that the initial triplet biexciton cannot undergo microscopic diffusive separation and, therefore, its fate can be examined more easily by spectroscopy. In this respect, weakly-coupled bichromophores are more interesting since the decorrelation[41] to a quintet state will likely occur on a relatively slow timescale. Such decorrelation is a necessary prerequisite for the evolution of an isolated triplet pair, where the two triplets act independently, and such behavior may not be possible for strongly-coupled chromophores. Understanding the decorrelation mechanism remains a critical goal.[42] A difficulty for establishing generic mechanisms and conclusions is that small changes in energetics can have important consequences for the triplet yield, with SEF switching between endergonic and exoergic processes. It has also become clear that the role of charge-transfer interactions is influenced by the nature of the chromophores and the local environment.[23] The same is true for any temperature dependence; this being further complicated by possible geometrical fluctuations. It is also apparent that optical spectroscopic methods, while being indispensable for establishing reaction rates, might not detect subtleties in the reaction mechanism that could be resolved by magnetic or vibrational techniques.[43] There is, throughout all of this impressive body of work, a general lack of strong evidence for the precise triplet excitation energies!

Here, we are concerned with understanding the details of iSEF occurring within a weakly-coupled, fluorene-bridged bichromophore constructed from TIPS-pentacene (TIPS = triisopropylsilylethynyl) terminals. Pentacene was one of the first molecules shown[44] to exhibit SEF and has been a cornerstone of contemporary studies. The parent molecule has limited solubility in common organic solvents and is susceptible to oxidative degradation.[45] Replacing pentacene with TIPS-pentacene (TIPS-P) solves both problems[46] and there have been numerous bis-TIPS-P derivatives reported over the past decade. A recent study[47] has described in full detail the photophysical properties of TIPS-P and provides quantitative data for both singlet- and triplet-excited states. An interesting feature of TIPS-P is that the inherent triplet yield is close to zero in the absence of a spin-orbit accelerant and therefore any triplet formation for the bichromophore must result from interaction between the terminals. Many of the earlier studies made with bis-TIPS-P derivatives focussed on molecular systems with relatively strong electronic coupling between the terminals.[26,29,35,48-51] In our case, the fluorene-based bridge minimizes contact between the two TIPS-P units.

The general consensus is that SEF with TIPS-P derivatives will be exoergic,[23] with the excitation energy of the triplet biexciton falling well below the energy of the excited-singlet state. There is, however, minimal experimental evidence to support this claim. The triplet energy of isolated TIPS-P was established[47] recently to be 7,940 ± 1,200 cm^{-1}, compared to the singlet excitation energy of 15,445 ± 100 cm^{-1}. This would indicate that the energetics for SEF are closely balanced. Phosphorescence studies made with relevant bichromophores[26,40] indicate a much lower triplet energy of 6,330 cm^{-1}. Although the origin of this latter emission is not clear, the implications are that iSEF involves an excess energy in the region of 2,700 cm^{-1}. The bichromophore studied here shows room-temperature phosphorescence, which can be used to establish the triplet excitation energy. With this latter value, photoacoustic calorimetry[52-56] (PAC) can be used to determine the yield of the various species responsible for the underlying enthalpy changes. This is the first time that PAC has been applied in the SEF field but it will be shown that the technique can provide important insight into the underlying processes.[47] It should be mentioned that a report has appeared[37] for the same bichromophore when subjected to indirect excitation using pulse radiolysis conditions.

EXPERIMENTAL

Samples of the target compound, PFP, and the parent, TIPS-P, were synthesized in-house and details are provided in the Supporting Information. Absorption spectra were measured with either a Shimadzu UV-2100 spectrophotometer or with a Hitachi U3310 spectrophotometer. Steady-state fluorescence measurements were recorded using a Horiba Fluorolog Tau-3 system with a water-cooled R2658P photomultiplier detector. Fluorescence quantum yields were measured using *meso*-tetraphenylporphyrin[57] as a standard (Φ_F = 0.11 in toluene). Cyclic voltammetry was made with a conventional 3-electrode system using a highly polished, glassy carbon working electrode. The counter electrode was a Pt wire and the reference electrode was an Ag/Ag^+ electrode maintained in acetonitrile. The background electrolyte was ammonium tetra-N-butylammonium perchlorate (0.2 M) and the solvent was freshly distilled CH_2Cl_2. An E600 potentiostat (CH Instruments) was used with a scan rate of 60 mV/s. Solutions were purged with N_2 before the experiment and maintained in an O_2-free environment throughout the scan.

Time-resolved fluorescence decay measurements were recorded with a time-correlated, single photon counting system, where excitation was made with a 635-nm short-pulse (FWHM = 90 ps) laser diode. A 1/4 meter Czerny-Turner emission monochromator was used to isolate fluorescence from scattered excitation light. Lifetime measurements were made after deconvolution of the instrumental response function using PTI Timemaster software. The temporal resolution of this set-up was ca. 60 ps. The solute absorbance was adjusted to be ca. 0.08 at 635 nm for all measurements and the solvent was first checked for the presence of emissive impurities.

Time-resolved absorption measurements were obtained with an Applied Photophysics LKS-70 system using a 4-ns pulsed Quantel Brilliant B Nd:YAG laser with the 1064 nm output frequency being doubled to 532 nm. The repetition rate of the laser was 10 Hz with the power varying from 1-50 mJ per pulse. Unless stated otherwise, the solution was de-oxygenated with a stream of dried N_2. Transient differential absorption spectra were collected point-by-point with 5 individual measurements

being averaged at each wavelength. Kinetic measurements were made at fixed wavelength with up to 256 individual traces being averaged and baseline corrected. The solution was refreshed periodically and all measurements were repeated at least three times. Data analysis was made using in-house software. Kinetic measurements made use of the Levenberg–Marquardt algorithm after signal averaging and, in each case, a range of time bases was used to extract the required triplet lifetime.

Improved temporal resolution was achieved using the pump-probe technique with an ultimate precision of 0.2 ps. The basic instrument has been described before[58] and used to study intramolecular SEF in bis-pentacene derivatives.[29,35] In brief, 100 fs pulses at 800 nm and at a repetition rate of 1 kHz were generated by a Libra F laser system (Coherent Inc.) and used to pump a Topas C OPA (Light Conversion Ltd.) so as to generate pump pulses at 600 nm. These pulses were used also to produce the white light probe. A time-resolved spectrometer (ExiPro, CDP Inc.) was used to collect a series of delayed transient absorption spectra over the desired wavelength range. Fresh solution was used for each laser shot and multiple spectra were averaged before analysis. Kinetic measurements were made by overlaying signals collected at different delay times at the same monitoring wavelength. Data analysis was made using in-house software. Molar absorption coefficients for transient species were determined from differential spectra recorded at 1 ps and at 1 ns, respectively, for excited-singlet and excited-triplet species. This was achieved using a model-based procedure and fitting spectra in the region of ground-state bleaching around 650 nm. At a time delay of 1 ns, the model assumes that there is only one triplet species present and that its concentration exactly matches the degree of ground-state bleaching.[59] The triplet species has no significant absorption at 650 nm and, after baseline correction, quantification of the spectra is straightforward.[60] This is not the case for the excited-singlet state, which displays pronounced, nonlinear absorption across the bleaching zone. There is also a small amount of stimulated emission that contributes to the apparent bleaching signal. Quantification required re-iteration of the ground-state absorption spectrum, the fluorescence spectrum and the observed differential absorption spectrum. Again the model assumed equal concentrations of excited-singlet state and ground-state bleaching but included the restriction that only one TIPS-P unit was bleached at the excited-singlet state level.

Photoacoustic calorimetry (PAC) experiments[61] employed a homemade front-face irradiation cell. As necessary, samples were saturated with N_2 for 20 min before starting the measurement. The sample, reference and solvent solutions were flowed separately (Kloehn syringe pump) through the 0.11 mm thick photoacoustic cell and exposed to pulses delivered with an OPO (Ekspla PG122/SH) pumped by the second harmonic of a nanosecond Q-switched Nd:YAG laser (Ekspla NL301G), working at a frequency of 10 Hz. The maximum energy per pulse was less than 1.0 mJ in all cases. The excitation wavelength was varied but kept close to the absorption peak of the solute. The photoacoustic waves were detected by a 2.25 MHz Olympus Panametrics transducer (model 5676), amplified by a preamplifier, recorded with a digital oscilloscope (Tektronix DPO7254C) and transferred to a PC for data analysis and storage. Analysis of the photoacoustic waves was performed with CPAC software.[62] In a typical PAC experiment, 200 waves were averaged for sample, reference and pure solvent using the same experimental conditions and with four different laser intensities. Neutral density filters were employed to vary the laser power. Measurements were made in de-aerated toluene using azulene as reference.[63]

For NIR emission studies, laser light (λ = 532 nm) from a Coherent Verdi V8 laser was focused onto the solid sample through an x63 water immersion objective lens (Leica, NA 1.2). A variable neutral density filter was used to attenuate the laser, such that 2 mW laser power was present at the beam focus. The emission signals were collected using the same objective lens (i.e., backscattered light) while a long pass dichroic mirror (Thorlabs DMLP1000) was used to reject all light below 985 nm. The signal was detected using a NIR spectrograph (Acton Research Company, Isoplane SCT-320) combined with an InGaAs array detector (Princeton Instruments, NIRvana 640). Acquisition times were typically 1 second. A 300 groove/mm grating, blazed at 1.2 microns, was used for all spectral measurements. The spectrograph was calibrated using the gas emission lines of a Mercury-Argon PenRay discharge lamp. The overall configuration of the spectrometer was similar to that described earlier.[47,64]

For liquid phase studies, the set-up was reconfigured to use pulsed laser excitation (10 ns, 532 nm, 10 Hz, 100 mW) with the sample being housed in a conventional plastic optical cuvette. Output from the laser was *cleansed* by passing through a band-pass filter (Thorlabs Inc.) centered at 532 nm and with a 10 nm bandwidth. A circular beam attenuator was used to restrict the average output power to ca. 80 mW. A laser collimator was used to generate an expanded beam of 3 mm diameter which was directed to an adjustable pinhole attached to one face of the sample cuvette. A dichroic mirror (Thorlabs Inc.) reflected the laser beam to the sample but allowed back transmission of photons in the NIR region. This emission was collected with a series of lenses and directed to a large area multimode fibre optic connected to the spectrograph. A long-pass filter with a cut-off of 1,100 nm was used to prevent further migration of residual fluorescence. The InGaAs array detector was equipped with thermoelectric cooling down to -90ºC and was operated in the free-running mode. The instrument was shielded from adventitious illumination and optimized using the zinc(II) tetraphenylporphyrin sensitized[65] formation of singlet molecular oxygen in air-equilibrated toluene. A typical NIR spectrum was compiled by averaging 25 acquisitions, each of 5 seconds.

RESULTS

Photophysical properties in toluene

Synthetic procedures for the target dye, the fluorene-bridged bis-TIPS-P derivative (PFP: Figure 1), are provided as part of the Supporting Information. The identity of the compound was confirmed by way of high-resolution NMR spectroscopy and mass spectrometry. The compound was found to have reasonable solubility in toluene, the solvent of choice for this work, and in most other organic solvents due to the presence of the TIPS groups.[46] A computerized model constructed for the essential core of the PFP module shows an extended geometry with the terminals held at an oblique angle (Figure 1). Although gyration around the bridge connection points ensures a wide variance in dihedral angles, the TIPS-P units cannot come into orbital contact and are kept apart by an edge-to-edge separation of ca. 10 Å. The transition dipole moment vectors are localized on the terminal pentacene chromophores, without any significant delocalization onto the fluorene-based bridge.

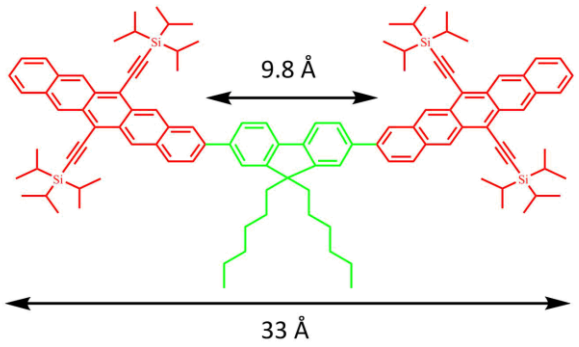

Figure 1. Computed molecular geometry for the target compound PFP. The mean dihedral angle between the fluorene-based bridge (green) and the terminal TIPS-P chromophores (red) is 36° as determined by *ab initio* DFT calculations (B3LYP/6-311++G/PCM) in $CHCl_3$ solution.**

The absorption spectrum recorded for PFP in toluene (Figure 2) differs somewhat from that recorded for the isolated control compound TIPS-P; direct comparison is made by way of Figure S12. Apart from a modest red shift, PFP exhibits additional higher-energy absorption bands at wavelengths below 450 nm (Figure S13). The molar absorption coefficient for the lowest-energy transition almost doubles from 23,250 M^{-1} cm^{-1} for TIPS-P at 643 nm to 43,000 M^{-1} cm^{-1} at 655 nm for PFP in toluene. The red shift is attributed to a small degree of extended conjugation imposed by electronic coupling to the spacer. Similar effects are apparent for other non-orthogonal bis-pentacene compounds.[23] The new absorption bands seen in the near-UV appear in the fluorescence excitation spectrum (Figure 2) and, therefore, are not due to impurities in the sample. Even so, samples were subjected to extensive TLC purification immediately before recording the spectra but this had no apparent effect on the absorption profile or kinetic measurements.

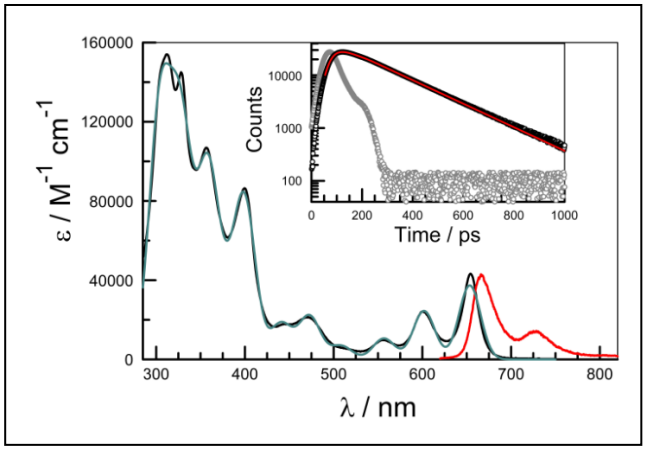

Figure 2. Comparison of normalized absorption (black curve) and fluorescence (red curve) spectra recorded for PFP in toluene. Also shown is the excitation spectrum (blue curve) after normalization at 600 nm. The insert shows an example of a time-resolved fluorescence decay curve recorded at 670 nm, with the fit to a lifetime of 192 ps (red curve) and with the instrumental response function shown as a grey curve.

Fluorescence is readily detected for PFP in dilute toluene solution and the spectral profile remains similar to that of TIPS-P, apart from a red-shift of 12 nm (Figure 2). The fluorescence maximum appears at 664 nm. A substantial decrease is observed for the emission quantum yield (Φ_F) relative to TIPS-P under identical conditions; Φ_F is measured to be 0.03 ± 0.002 in dilute toluene solution compared to a value of 0.75 found for TIPS-P.[47] In toluene at room temperature, the excited-singlet state lifetime (τ_S) is 200 ± 15 ps, as measured by time-correlated, single photon counting. Again, this parameter is substantially shortened relative to that of TIPS-P (τ_S = 14 ± 0.5 ns),[47] indicating the introduction of a new nonradiative channel for PFP that competes effectively with radiative decay. The singlet excitation energy can be equated to the crossover point between normalized absorption and fluorescence spectra, which is 15,165 cm^{-1} (i.e., 1.88 eV).

Low-temperature fluorescence measurements made in either methylcyclohexane or 2-methyltetrahydrofuran show a red-shift of ca. 10 nm and a sharpening of the spectrum upon stepwise cooling from room temperature to 80K (Figure S12). The fluorescence yield was corrected for solvent contraction[66] and spectral shifts at the excitation wavelength in order to examine how the nonradiative rate constant depends on temperature. However, the fluorescence quantum yield was found to be insensitive to temperature over this range (Figure S14), meaning that the new deactivation channel is activationless. This finding is consistent with singlet-exciton fission. For example, Friend *et al*.[67] reported activationless SEF over a wide temperature range for thin films of tetracene. There is, in fact, no obvious reason for singlet-exciton fission to require an activation energy – although the absence of an activated barrier does not by itself prove that the enhanced nonradiative decay observed for PFP is primarily due to iSEF.

Excitation of PFP in toluene with a short laser pulse (FWHM = 0.2 ps) at 600 nm generates the transient differential absorption spectrum displayed in Figure 3a. At the earliest times, the most notable features include bleaching of the 0,0 band at 655 nm and a pronounced absorption band centered at around 460 nm. Multi-variate curve fitting[68] indicates that, on early timescales, the full spectral profile can be well described in terms of ground-state bleaching and concomitant absorption by a single transient species. The differential absorption spectrum recorded for delay times of a few ps bears only a superficial resemblance to that reported[47] for the excited-singlet state of TIPS-P in toluene (Figure S15). In particular, the spectrum derived for PFP is broadened, especially in the lower energy region around 530 nm, although the peak of the differential spectrum is close to that for TIPS-P. On longer timescales, the absorption band at 460 nm is replaced with a broad absorption profile centered at ca. 530 nm and is accompanied by significantly increased bleaching of the ground-state absorption bands. Isosbestic points are preserved at 490 and 560 nm (Figure 3a). This second transient species, which hardly decays on the 6-ns temporal window available with this instrument, is assigned to a triplet species.[6] Global analysis[59,60,68] indicates that the excited-singlet state decays via exponential kinetics with a lifetime of 190 ± 20 ps (Figure 3), in excellent agreement with the fluorescence lifetime. Thus, despite the disparity in absorption spectra, we are able to assign the initial species to the locally-excited singlet state of the bichromophore. Under the conditions of the experiment, there is little likelihood for dual excitation of PFP.

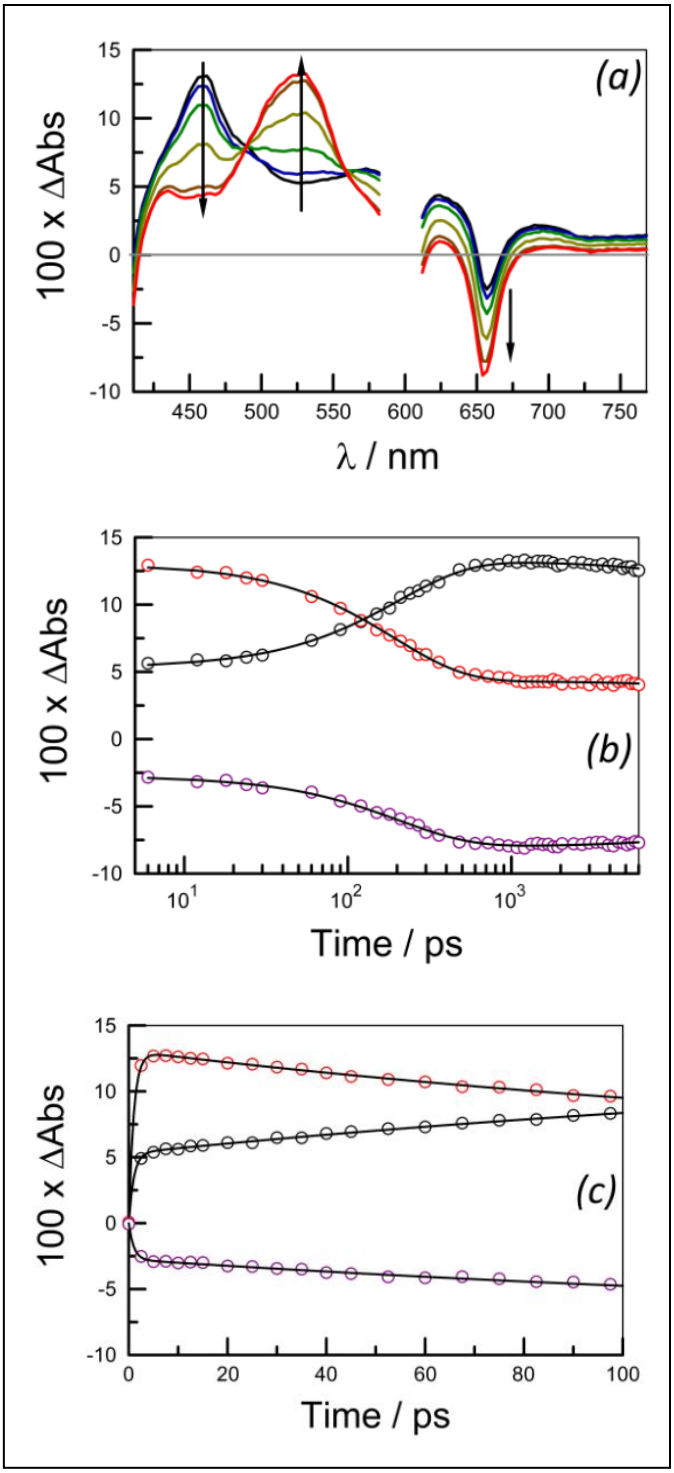

Figure 3. (a) Selected transient absorption spectra recorded after laser excitation of PFP in toluene at 600 nm. The arrows indicate the course of increasing time delay. Individual spectra were recorded at delay times of 3.5, 20, 65, 175, 545 and 1,745 ps. (b) Kinetic traces recorded at 459 nm (red curve), 530 nm (black curve) and 655 nm (indigo curve) and covering the timescale from 1 ps to 6 ns. (c) Kinetic traces recorded over a timescale of 1 to 100 ps and monitored at 459 nm (red curve), 530 nm (black curve) and 655 nm (indigo curve). In all cases, the nonlinear least-squares fit to the experimental data corresponds to the value reported in the text.

The triplet species absorbing at 530 nm is also observed following excitation with a 4-ns laser pulse (Figure 4). The same differential absorption spectrum is observed, irrespective of laser intensity or excitation wavelength, but again this differs from that characterized[47] for the triplet state of TIPS-P in toluene (Figure S16). Analysis on the microsecond timescale indicates that the triplet species decays via first-order kinetics with a lifetime of 8 ± 2 μs in de-aerated toluene (Figure 4); in air-equilibrated toluene, the triplet lifetime is shortened to 1.25 ± 0.2 μs (Figure S17). The ground-state is recovered during this process but the transient differential absorption spectrum undergoes minor changes during a few hundred ns or so. Essentially, these changes amount to a small shift of the absorption maximum from 530 nm to around 520 nm, which occurs with a mean lifetime of 135 ± 20 ns in de-aerated toluene (Figure 4).

Commensurate with this relatively fast triplet decay, the ns-laser flash photolysis records indicate the appearance of delayed fluorescence[9] following excitation at 532 nm. This emission is very weak but displays a similar spectral profile to that recorded earlier for spontaneous fluorescence (Figure S21). The intensity depends linearly on incident laser power while the emission half-life is independent of the initial triplet concentration. These factors, together with the relatively fast timescale and low solute concentration, indicate that the origin of the delayed emission is intramolecular triplet-triplet annihilation (TTA).[9] However, the lifetime derived for the crop of delayed fluorescence (τ_{DF} = 50 ns) is less than one-half that recorded for triplet decay (τ_{TTA} = 135 ns) under the same conditions (Figure S22).[69] While TTA is common for tetracene,[70,71] where SEF is endergonic,[67] it has rarely been reported for pentacene-based systems. Room temperature TTA has been described for an orthogonal bis-pentacene derivative[72] and for thin films of pentacene.[16]

It might be stressed that the differential absorption spectra recorded for PFP differ somewhat from those recorded for TIPS-P.[47] These spectral disparities are attributed to a modest degree of electronic coupling between the terminal chromophore and the fluorene-based bridge. The main consequence of this mutual interaction is that molar absorption coefficients determined for TIPS-P cannot be used for PFP. Earlier work carried out with TIPS-P in toluene has established[47] the differential molar absorption coefficient for the excited-singlet state at 455 nm as being 37,200 M^{-1} cm^{-1}. This value is similar to that (ε_{455} = 38,250 M^{-1} cm^{-1}) found using pulse radiolysis methods.[37] Iterative reconstruction[68] of the corresponding differential spectrum recorded for PFP, together with the ground-state absorption spectrum and the room-temperature fluorescence spectrum, was applied to obtain ε_{459} for PFP. The derived value of 33,800 ± 3,500 M^{-1} cm^{-1} is lower than that for TIPS-P, but the spectrum is notably broadened so that the overall oscillator strengths are more comparable. Taking into account the fact that only one of the terminal chromophores can be promoted to the excited-singlet state, the molar absorption coefficient of the ground-state chromophore at 655 nm was taken as being one-half that of the bichromophore.

It was reported[47] earlier that triplet formation for TIPS-P was insignificant in the absence of a spin-orbit promotor. This being the case, production of triplet species for PFP must arise from a non-conventional route. Assuming this to be iSEF, the initially formed triplet species should be the spin-correlated, triplet biexciton[73] possessing an overall spin multiplicity of unity.[74] For weakly coupled triplet biexcitons, spin decorrelation has been

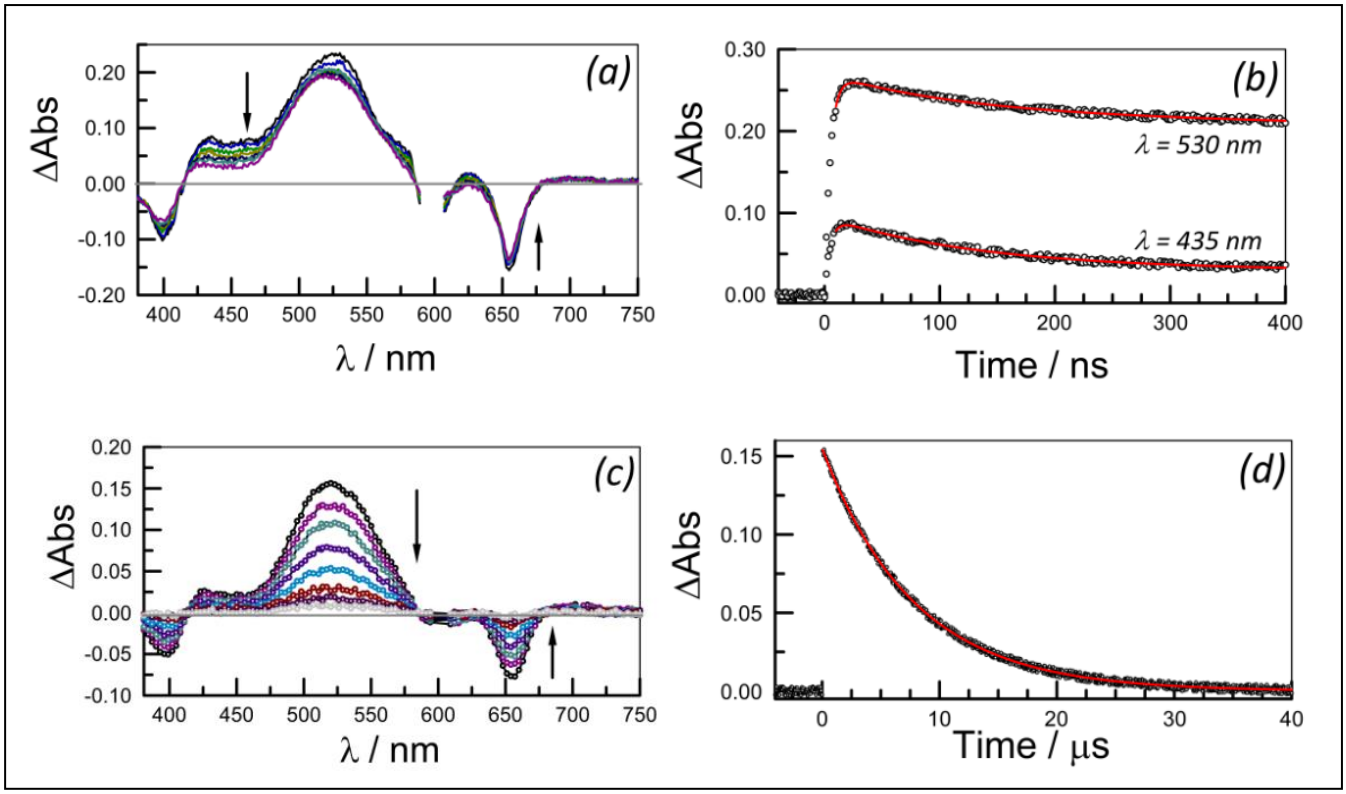

Figure 4. (a) Transient differential absorption spectra recorded after laser excitation of PFP in de-aerated toluene with a 4-ns laser pulse delivered at 600 nm. The arrows indicate the direction of increased delay time. Individual spectra were recorded at time delays of 10, 40, 70, 100, 150, 200 and 300 ns. (b) Kinetic traces recorded over 400 ns for the experiment reported in part (a) and with monitoring wavelengths of 530 and 435 nm. The best fits to the experimental data are shown as red lines and give a mean lifetime of 135 ns. (c) Corresponding spectra recorded on longer timescales; individual spectra being recorded at delay times of 0.04, 1.48, 2.96, 5.36, 8.24, 13.9, 16.4 and 24.2 μs. (d) Kinetic trace recorded at 525 nm for the experiment reported in part (c). The best fit to the experimental data is shown as a superimposed red line and corresponds to a lifetime of 7.8 μs.

reported[23] to occur on the ns timescale, according to the degree of electronic communication, to generate the triplet biexciton having higher spin multiplicity. Such spin conversion is accompanied by subtle absorption spectral changes, notably in the red region,[6,23] but is probably best monitored using time-resolved EPR spectroscopy.[75-77] In the case of PFP, there are minor absorption spectral changes in the region around 530 nm together with a more significant absorption change around 430 nm; spectral variations occurring over a few hundred ns in both cases (Figure 4). The fractional decay depends on monitoring wavelength. We assign this step, for which the mean lifetime is 135 ± 20 ns, to decorrelation of the triplet biexciton.[23] The net product is a triplet species, having a lifetime of 8 ± 2 μs, which retains similar absorption spectral features to the initial biexciton. Given its long lifetime, the final transient species is believed to be an independent pair of triplet states.[78] This latter lifetime remains essentially independent of temperature over the range 10-55 °C. In contrast, decay of the spin-correlated, triplet biexciton is activated and shows linear Arrhenius behavior over a modest temperature range in toluene (Figure S20). This corresponds to an activation energy of 21.5 kJ/mol and a pre-exponential term of 8×10^{10} s^{-1}.

Spectral reconstruction[68] using transient differential absorption spectra recorded on timescales between 1 and 6 ns have been used to derive the differential molar absorption coefficient for the initial (i.e., spin-correlated) triplet biexciton. With ε_{655} = 43,000 M^{-1} cm^{-1} for the ground state, a value for ε_{530} of 64,710 ± 4,000 M^{-1} cm^{-1} is reached for the triplet species. Here, the excited state has minimal absorption in the region of ground-state bleaching; a situation that greatly aids determination of the absorption coefficient. It should be re-emphasized at this point that the differential absorption spectrum assigned to the correlated triplet biexciton shows important differences from that reported[47] for TIPS-P (Figure S16). Significant differences also exist for molar absorption coefficients measured at the respective maxima. The value[47] for TIPS-P is 81,500 M^{-1} cm^{-1}, which is more than twice the value found for PFP on a per triplet basis. Furthermore, the value found for the initial triplet biexciton is much lower than that measured by triplet sensitization under conditions that permit only a single triplet species to be associated with a PFP molecule. This latter situation is easily accomplished under pulse radiolysis conditions to give ε_{530} of 71,000 ± 6,000 M^{-1} cm^{-1}.[37]

Comparing mean absorbance values for excited-singlet and triplet species at 459 nm and 530 nm, measured at 5 ps and at 1 ns respectively, can now be used to establish the relative yield of triplet species. In toluene, the average yield for population of the spin-correlated triplet biexciton, determined on the basis of the above-derived molar absorption coefficients, is 65 ± 7%. The same value is recovered by comparing the magnitudes of

the ground-state bleach at 655 nm at these same time delays; this gives a relative triplet yield of 130%. This is a considerable enhancement of the triplet population relative to the parent TIPS-P but falls well short of values reported for related closely-coupled bichromophores.[23] Furthermore, there are likely to be additional losses as spin decorrelation leads to evolution of the independent triplet pair. Complete decorrelation requires a few hundred ns but the transient absorption spectral data do not permit an accurate determination of the quantum yield for formation of the independent triplet pair; the main uncertainty being lack of detailed knowledge of molar absorption coefficients for the respective species. The overall situation is illustrated by way of Scheme 1.

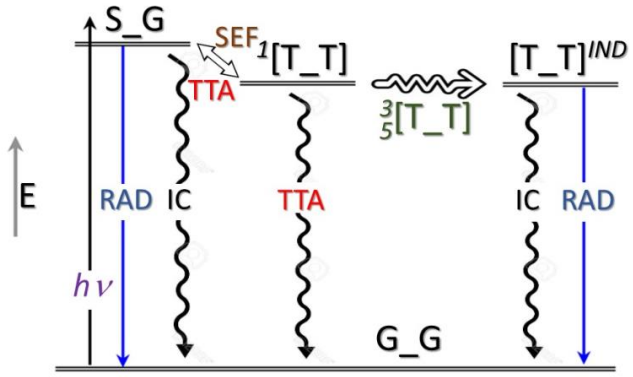

Scheme 1. Generic outline proposed to explain the photophysics for PFP in toluene. Excitation of the ground state (G_G) leads to formation of the singlet-excited state (S_G) where only one of the two TIPS-P units is excited. This species decays quickly to reform the ground state via internal conversion (IC) and, by way of iSEF, to generate the correlated triplet biexciton (^{1}[T_T]). The latter species undergoes triplet-triplet annihilation (TTA) in competition to decorrelation to form the independent triplet pair ([T_T]^{IND}). Spin decorrelation is assumed to proceed through triplet and quintet species. During TTA from ^{1}[T_T], repopulation of S_G must occur since a small amount of delayed fluorescence is observed. A key assumption of this scheme is that the various triplet biexcitons share a similar excitation energy.

Phosphorescence spectroscopy

An unexpected result from our analysis of the transient absorption spectral records for PFP in de-aerated toluene is the apparent observation of intramolecular TTA leading to delayed fluorescence.[9,69] If correct, this observation requires the triplet excitation energy to be not significantly less than one-half that of the corresponding excited-singlet state. The latter (E_S) can be established with good precision as being 15,165 cm^{-1} (i.e., 1.88 eV). In order to determine the corresponding triplet energy (E_T), attempts were made to detect emission in the near-IR region that might be attributable to phosphorescence. To avoid artefacts, two independent measurements were made using dissimilar experimental conditions.

Firstly, a small aliquot of solid PFP was placed on a microscope cover slip and immersed in a drop of water. The sample was illuminated with a diode-pumped, solid-state laser emitting at 532 nm; the power being kept below 2 mW to prevent sample ablation. A 985-nm cut-off filter was used to reject most of the residual fluorescence and the emission spectrum was recorded as far as 1,550 nm. The background signal was recorded and subtracted using a segment of the cover slip without sample. An acquisition time of 1 s was applied. Apart from enhanced background signal, attributed to scattered fluorescence, sharp emission peaks are seen at 1,372 and 1,479 nm (Figure 5a). This emission was detected only under laser excitation and was not the result of photolysis. The same spectrum was observed for different samples of PFP but, under the same conditions, could not be detected for solid TIPS-P.[47] The sharp spectrum is assigned to phosphorescence from PFP. The spacing between the peaks ($h\omega$ = 530 cm^{-1}) and the Huang-Rhys factor[79] (S = 0.56) appear reasonable for an aromatic polycycle. The triplet energy, taken simply from the peak at 1,372 nm, can now be set at 7,290 cm^{-1} (i.e., 0.90 eV).

In the second experiment, a solution of PFP in de-aerated toluene was exposed to a train of 4-ns laser pulses delivered at 532 nm. Here, the emission spectrum consists of background fluorescence and a pair of relatively sharp peaks at 1,370 and 1,455 nm (Figure 5b). The sharp spectrum, assigned to phosphorescence from PFP, is in good agreement with that observed for the solid sample. The spacing between the peaks, which corresponds to a low-frequency vibronic mode of 430 cm^{-1}, and the Huang-Rhys factor (S = 0.90)[79] differ slightly from those found for the solid sample but this might simply reflect the disparate environments. It is difficult to assign this emission to anything other than phosphorescence from the independent triplet pair. This leads to an estimate for the mean triplet energy for the biexciton of 14,580 ± 200 cm^{-1}.

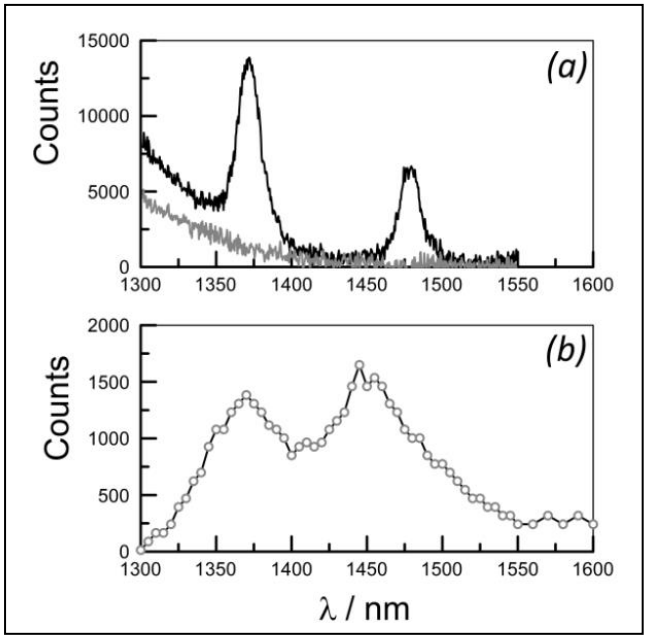

Figure 5. (a) Near-IR luminescence spectra recorded for solid-state samples of PFP (black curve) and TIPS-P (grey curve) with excitation at 532 nm. (b) Corresponding spectrum recorded for PFP in de-aerated toluene solution under dilute conditions.

Photoacoustic calorimetry

A complex picture is emerging for the photophysical properties of PFP in dilute toluene solution. This situation arises because branching seems to occur at each of the critical points

Table 1. Compilation of the experimental data derived from the PAC experiments made with PFP in de-oxygenated toluene at room temperature. Refer to Scheme 2 for further information about the various processes.

Parameter	Expt #1	Expt #2	Expt #3	Expt #4	Mean
[PFP] / μM	2.1	4.4	8.0	9.8	
λ_{EX} / nm	655	644	650	647	
E_λ / cm^{-1}	15,265	15,530	15,385	15,455	
ϕ_1	0.385 ± 0.004	0.501 ± 0.029	0.395 ± 0.005	0.470 ± 0.020	0.44 ± 0.05
ϕ_2	0.110 ± 0.019	0.171 ± 0.005	0.147 ± 0.007	0.155 ± 0.008	0.15 ± 0.04
τ_2 / ns	204 ± 17	136 ± 5	122 ± 4	117 ± 4	
ϕ_3	0.505 ± 0.023	0.328 ± 0.034	0.458 ± 0.012	0.375 ± 0.028	0.417 ± 0.095
ϕ_{IC} [a]	0.357	0.469	0.362	0.439	0.41 ± 0.06
Φ_{IND} [b]	0.53	0.35	0.48	0.40	0.44 ± 0.09
E_{TT} / cm^{-1} [c]	14,445	11,920	14,320	12.600	13,320 ± 1,300
P_{DEC} [d]	0.82 (0.82)	0.66 (0.66)	0.75 (0.76)	0.73 (0.71)	0.74 ± 0.08
P_{DEC} [e]	0.74	0.60	0.66	0.66	0.66 ± 0.08

(a) Obtained from evaluation of Equation 1 with E_{TT} fixed at 14,580 cm^{-1}. (b) Obtained from evaluation of Equation 2 with E_{TT} = 14,580 cm^{-1}. (c) Derived from Equation 1 but using Φ_{SEF} = 0.65. (d) Calculated without repopulation of S_G using Equation 3, with values from Equation 7 in parenthesis. (e) Calculated with recycling (<n> = 2) using Equation 9.

leading to evolution of an independent pair of triplet states. Our estimate of the triplet excitation energy means that iSEF is mildly exoergic while optical absorption spectroscopy does not facilitate detailed analysis of the decorrelation step.[23] Our observation of delayed fluorescence, although very weak, ensures that there will be some degree of cycling between the excited states as happens for thermally-activated, delayed fluorescence.[80-82] In searching for a possible means by which to refine the proposed reaction pathway, our attention was drawn to the application of photoacoustic calorimetry,[47] which gives information on the quantity of heat released by way of radiationless deactivation of an excited species.[52-56] For the experiment in question, direct excitation of PFP in de-aerated toluene with a 4-ns laser pulse should ensure formation of the triplet biexciton by way of fast iSEF. The time resolution set by the 2.25 MHz transducer covers the range 20 ns to 1 μs.[53] This allows isolation of three separate enthalpy changes which can be distinguished in terms of their respective timescale (Figure 6). We refer to these steps as being "very fast", "fast" and "slow". The experimental data are compiled in Table 1 and analysis is made according to Scheme 1. The latter is redrawn as Scheme 2 in a form that reflects the photoacoustic experiments in a more convenient manner.

In summary, the "very fast" enthalpy change must be associated with relaxation of the excited-singlet state (S_G) of PFP to form the spin-correlated, triplet biexciton (^{1}[T_T]). This is the only process that occurs within the pertinent time window and that is likely to give rise to a significant heat release. The "very fast" processes provide the first fraction of heat detected (ϕ_1) (Scheme 2). The "fast" processes account for the second fraction of released heat (ϕ_2), which must occur within the instrumental time window. The underlying photophysical steps include TTA, radiationless decay of ^{1}[T_T] and the concomitant decorrelation of the biexciton. The "slow" processes are not detected by our set-up but correspond to the enthalpy retained by the long-lived, independent triplet pair. The experiment allows detection of the fractions of the excitation energy (E_λ) associated with the first two steps, thereby providing the third fraction by difference. Excitation was made at different wavelengths around 650 nm and the system was calibrated by reference to azulene.[63]

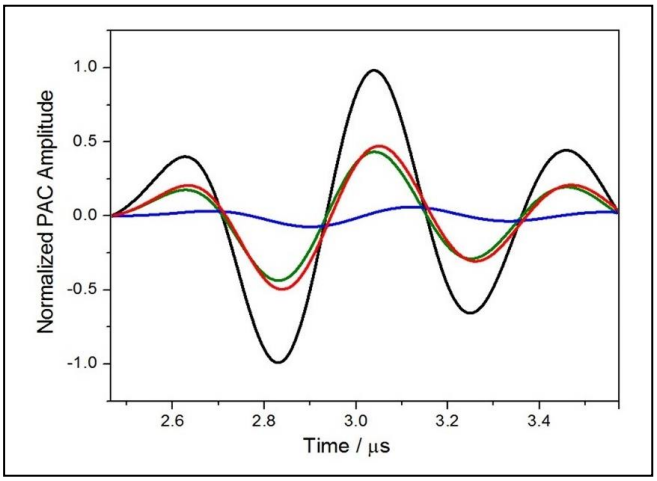

Figure 6. Examples of photoacoustic waves associated with the different components identified in the text and for which the values are collected in Table 1. The black curve refers to the azulene standard while the red curve shows the total photoacoustic wave recorded for PFP. The first component identified for PFP, ϕ_1 = 0.44 and τ_1 = 1 ns, is shown as an olive curve. The second component, ϕ_2 = 0.15 and τ_2 = 145 ns, is shown as a blue curve.

The first point to note is that the fraction of excitation energy released in the "very fast" step (ϕ_1) is rather high and amounts to more than 40% of the energy input (Table 1). A small contribution to this enthalpy change can be assigned to intramolecular vibrational relaxation (IVR) within the excited-singlet state manifold since the excitation energy, E_λ, slightly exceeds the

energy of the relaxed excited-singlet state (E_S = 15,165 cm^{-1}). This is a minor heat release, however, that makes but a small contribution towards the overall enthalpy change ($\Delta H_1 = \phi_1 \times E_\lambda \approx 6{,}750 \pm 1{,}300$ cm^{-1}). A second contributor is the heat released on conversion of S_G to the spin-correlated triplet biexciton. The energy of the latter species (E_{TT} = 14,580 cm^{-1}) is assumed to equal twice the phosphorescence energy. Again, this process will release only a relatively small quantity of heat since the two states are quite close in energy, regardless of the precise magnitude of E_{TT}.

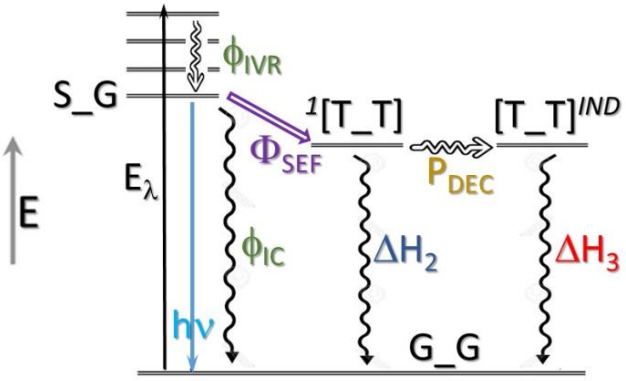

Scheme 2. Representation of the overall enthalpy changes that follow from excitation of PFP in toluene with a laser pulse at wavelength λ. The enthalpy is released to the solvent in three steps, which correspond to ΔH_1, ΔH_2 and ΔH_3, while the sum of these enthalpy changes equals the excitation energy E_λ. The model does not allow for the expected energy change associated with decorrelation of the triplet biexciton, which is assumed to be negligible.

To give a quantitative account of ΔH_1 it is necessary to invoke a radiationless process, such as internal conversion to the ground state. This step (Scheme 2) would inject a significant amount of heat into the solvent reservoir on an appropriate timescale. Furthermore, the simplest scheme partitions deactivation of S_G between iSEF (Φ_{SEF}) and internal conversion (Φ_{IC}) such that the sum of the two quantum yields must equal 0.97 (i.e., 1-Φ_F). Now, solving Equation 1 allows estimation of Φ_{IC} as being 0.41 ± 0.06, such that the probability for iSEF in this system has to be close to 60% (Table 1). This latter estimate is in very good accord with that derived from the transient absorption spectral studies (Φ_{SEF} = 0.65) and, taking into account the respective error limits, the two measurements overlap nicely.

Re-evaluation of Equation 1 but using the experimental value of Φ_{SEF} = 0.65 allows estimation of the triplet energy for the spin-correlated biexciton of 13,320 ± 1,300 cm^{-1} compared to the *presumed* experimental value of 14,580 cm^{-1}. This procedure places all the associated error onto the final term in the expression, which concerns the difference between two similarly large numbers. The result is a loss of precision although the derived E_{TT} is closer to our original expectation!

$$\Delta H_1 = \phi_1 E_\lambda = (E_\lambda - E_S) + \phi_{IC} E_S + \Phi_{SEF}[E_S - E_{TT}] \quad (1)$$

The residual enthalpy (ΔH_3) that dissipates on the μs timescale can be attributed to deactivation of the independent triplet pair (Table 1). Within the confines of Scheme 2, this species evolves from spin decorrelation of the initially formed triplet biexciton and is believed responsible for the observed phosphorescence. The residual enthalpy ($\Delta H_3 = \phi_3 \times E_\lambda \approx 6{,}410 \pm 900$ cm^{-1}) accounts for a substantial fraction of the initial excitation energy, thereby indicating that the long-lived triplet species is formed in respectable yield. The energy of this species (E_{TT} = 14,580 cm^{-1}) can be recovered from the phosphorescence measurements while the overall quantum yield for generation of the independent triplet pair can be expressed as Φ_{IND} (Equation 2). It should be noted that Φ_{IND} is a global term that takes into account any repopulation of S_G during TTA. Analysis of Equation 2 allows determination of Φ_{IND} as being 0.44 ± 0.09 (Table 1). The finding that Φ_{IND} is much less than Φ_{SEF} is especially significant because it provides firm indication for a nonradiative decay channel that competes with spin decorrelation of ^{1}[T_T]. The nature of this latter deactivation step cannot be established solely on the basis of the PAC results but two limiting cases can be identified.

$$\Delta H_3 = \phi_3 E_\lambda = \Phi_{IND} \times E_{TT} \quad (2)$$

$$\Phi_{IND} = \Phi_{SEF} \times P_{DEC} \quad (3)$$

$$P_{DS} = 0.5(1 - P_{DEC}) \quad (4)$$

$$\Phi_{IND} = (\Phi_{SEF} \times P_{DEC})[1 + [P_{DS}\Phi_{SEF}] + [P_{DS}\Phi_{SEF}]^2 \dots] = \left(\frac{\Phi_{SEF} \times P_{DEC}}{1 - [P_{DS}\Phi_{SEF}]}\right) \quad (5)$$

Firstly, internal conversion might compete with spin decorrelation. This process would restore the ground state without repopulation of S_G. In this case, Equation 3 holds, where P_{DEC} refers to the fractional probability that ^{1}[T_T] undergoes spin decorrelation to ultimately form the independent triplet pair. Under these limiting conditions, P_{DEC} can be estimated as being ca. 0.75; that is to say that internal conversion from ^{1}[T_T] to G_G occurs with a probability of 25%. Secondly, in an effort to account for the observed delayed fluorescence, it is proposed that the competing nonradiative channel amounts to conventional triplet-triplet annihilation (TTA).[9] This situation has been observed for thermally-activated, delayed fluorescence in certain organic emitters.[80-82] In this case, the decay channel will form equal populations of the ground state, G_G, and the excited-singlet state, S_G;[83] the fractional probability for repopulation of S_G is abbreviated as P_{DS} and can be obtained from P_{DEC} (Equation 4). The latter excited state will recycle and give a further crop of the independent triplet species. Within this limiting case, Equation 5 will hold and there will be a decrease in P_{DEC} compared to the non-cycling case. Indeed, evaluation of Equation 5 gives P_{DEC} = 0.66. The crop of triplet species decreases rapidly with increasing cycle number and, given the magnitude of the experimental errors, we have restricted our analysis to two successive repopulations of S_G (see below).

The challenge now is to account for the "fast" enthalpy release (Table 1), which makes a modest contribution to the overall total. This step (ΔH_2) occurs with a lifetime (τ_2) in the order of 100-200 ns and, in terms of Scheme 2, is associated with the TTA and spin decorrelation processes. For simplicity, we first consider the case where recycling does not occur but competitive internal conversion depletes ^{1}[T_T] during spin decorrelation to the independent triplet species. This leads to Equation 6. Within our model, the decorrelation step cannot contribute significantly to the overall enthalpy change since the initial and final excitation triplet energies must be similar (i.e., $\Delta E_{TT} \approx 0$); this is an over simplification but the experimental E_S and E_T values leave little room for a stepwise gradation in triplet energies for the various biexciton species. Accordingly, the only significant contributor to the "fast" enthalpy change is vibrational relaxation of ^{1}[T_T] to restore the ground state (Equation 7).

Subsequent analysis, making use of Φ_{SEF} = 0.60 and E_{TT} = 14,580 cm^{-1}, leads to a mean value for P_{DEC} of 75%. (Table 1) This is in excellent agreement with that determined above from Equation 3.

$$\Delta H_2 = \phi_2 E_\lambda = (\Phi_{SEF} P_{DEC} \Delta E_{TT}) + \{\Phi_{SEF}(1 - P_{DEC}) E_{TT}\} \quad (6)$$

$$\Delta H_2 = \phi_2 E_\lambda \approx \Phi_{SEF} \times (1 - P_{DEC}) \times E_{TT} \quad (7)$$

$$\langle n \rangle \approx \frac{\Phi_{SEF} \times P_{DEC}}{1 - \Phi_{SEF} \times P_{DEC}} \quad (8)$$

$$\Delta H_2 = \phi_2 E_\lambda \approx 0.97 \Phi_{SEF} \{P_{DS} E_{TS} + \Phi_{IC} P_{DS} E_S + P_{DS}^2 \Phi_{SEF} E_{TS} + P_{DS}^2 \Phi_{SEF} \Phi_I E_S + P_{DS}^3 + \Phi_{SEF}^2 T_{TS}\} \quad (9)$$

Re-population of the excited-singlet state from ^{1}[T_T] means that the enthalpy change can be considered to occur in successive waves,[80] although in reality heat release will be continuous, according to the recycle number. Such behavior is already known from studies made with thermally-activated, delayed fluorescence.[80-82] The mean recycle number, <n>, can be approximated as in Equation 8 from which subsequent evaluation indicates that only two cycles need be considered. Consequently, the quantity of heat released into the system during the available time window, with due allowance for recycling, can be expressed as in Equation 9; where $E_{TS} = E_{TT}-(E_S-E_{TT})$. Here, we ignore any heat generated by the actual decorrelation step and assume that heat released during spin decorrelation arises entirely from TTA. As above, the latter process is partitioned equally between repopulation of S_G and G_G.[83] The observed enthalpy change, ΔH_2, can be used to determine the magnitude of P_{DEC} in the event of recycling. The final result is that the mean value for P_{DEC} is 0.66 ± 0.08 (Table 1). This agrees fully with that derived from Equation 5 and, as expected, is lower than that predicted in the absence of recycling.

Table 2. Solvent dependence on singlet decay rate and triplet yield of PFP in dilute solution, obtained from transient absorption spectroscopy.

Solvent	ε_S [(b)]	k_D / 10^9 s^{-1} [(c)]	Φ_{SEF} [(d)]	τ_{IND} / μs [(e)]
C_6H_{12}	2.02	3.6	68	6.3
C_7H_8	2.38	5.0	65	8.0
$CHCl_3$	4.81	5.9	72	5.8
THF [(a)]	7.52	7.7	80	NA
C_6H_5CN	26.0	10.0	93	5.5

(a) Tetrahydrofuran. (b) Static dielectric constant. (c) Rate constant for total deactivation of the excited-singlet state. (d) Quantum yield for formation of the spin-correlated triplet biexciton referenced to toluene solution. The calculation assumes that any absorbance present at 1 ns delay is due to the triplet biexciton. (e) Lifetime of the independent triplet species recorded at 520 nm.

Effect of solvent polarity

Some earlier studies[23] have suggested a step-wise mechanism for SEF in which a charge-transfer state functions as an intermediate species on the way to formation of the spin-correlated, triplet biexciton. This has become known as the "indirect SEF mechanism".[84,85] It is well established that the energy of an intramolecular charge-transfer state (ICTS) can be tuned by way of dielectric environmental effects,[86] such as changing the solvent polarity,[87] which should not affect the energetics for iSEF. Of course, if the energy of the ICTS is lowered too much, this state will become a trap for the excitation energy and a barrier will be imposed for the second step that leads to evolution of ^{1}[T_T]. In certain systems[88] it has been shown that increasing solvent polarity leads to enhanced rates of SEF but the role, if any, of the ICTS seems highly sensitive to the molecular structure.[23]

Transient absorption spectroscopic measurements were made with PFP in a few solvents of increasing dielectric constant (ε_S) where the rate constant (k_D) for deactivation of the excited-singlet state can be equated to the inverse fluorescence lifetime (τ_S) (Table 2). It is seen that k_D exhibits a shallow dependence on solvent polarity, which seems consistent with an ICTS contributing towards deactivation of the S_G state. The appearance of the transient absorption spectrum is not ostensibly altered in the different solvents, except for cyclohexane where the absorption bands are sharper (Figure S19), and the decay kinetics remain first order in all cases (Figure S18). Also collected in Table 2 are the quantum yields (Φ_{SEF}) for formation of the spin-correlated, triplet biexciton. The latter were determined directly from the ratio of absorbance values measured at 1 ps and at 1 ns for excited-singlet and triplet states, respectively, using molar absorption coefficients reported for toluene. The transient absorption records show the enhanced decay rates found in polar solvents are matched by increasing yields of triplet species. Furthermore, the solvent effects can be explained[89] satisfactorily using an empirical dielectric saturation model as illustrated by Figure 7 (see Supporting Information for details). This behavior is fully consistent with an intermediary role for charge-transfer state.

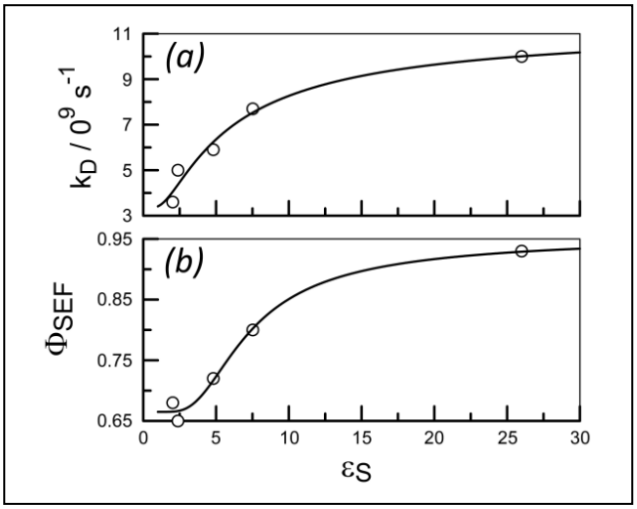

Figure 7. Effect of solvent dielectric constant on (a) the global rate of deactivation of S_G at room temperature and (b) the quantum yield for formation of the spin-correlated, triplet biexciton. The solid line drawn through the data points corresponds to an empirical fit to a dielectric saturation model (see Supporting Information).

The apparent yield of ^{1}[T_T] approaches 100% in benzonitrile solution at room temperature (Table 2). This finding indicates that the rate of iSEF increases substantially relative to internal conversion in the polar solvent. Thus, the ICTS intermediate, if formed, promotes SEF without affecting the rate of internal conversion. There is also a small solvent effect on spin decorrelation of the initial triplet biexciton; specifically, the lifetime of ^{1}[T_T] decreases from 135 ns in toluene to 100 ± 8 ns in benzonitrile at room temperature. In deoxygenated mineral oil, this lifetime increases to 220 ns. In marked contrast, the

lifetime of the independent triplet pair (τ_{IND}) is quite insensitive to solvent polarity and in de-aerated benzonitrile has a value of 5.5 ± 1.0 μs; in outgassed mineral oil τ_{IND} is 6.0 μs The overall effect of increased solvent polarity, at least in the case of PFP, is to favor SEF over internal conversion without seriously shortening the lifetime of the final triplet species. *This is a highly encouraging result.*

DISCUSSION

Relative to TIPS-P,[47] the bichromophore PFP shows weak fluorescence but greatly enhanced triplet formation in nonpolar solvents at room temperature. The fluorescence yield is insensitive to changes in temperature. These are the hallmarks of intramolecular singlet exciton fission (iSEF) and PFP can be added to the list of TIPS-P-based bichromophores known to undergo triplet multiplication.[23] The molecular structure is such that the terminal TIPS-P units cannot come into orbital contact (Figure 1) and there is no spectroscopic or kinetic evidence to implicate excimer fluorescence.[90,91] Nonetheless there are noticeable spectral shifts for PFP compared to TIPS-P. These perturbations are especially important at the excited-state level and amount to a significant broadening of the excited-state absorption transitions. This effect is ascribed to partial delocalization of the excited-state wave-function onto the bridging fluorene unit, introducing nebulous character at the interface. Similar effects might be relevant for other symmetrical bichromophores that display enhanced triplet formation. The signature for such electronic delocalization, at least in terms of absorption spectroscopy,[9] is likely to be broadened and red-shifted optical transitions but there has not been a systematic examination of this effect.

A critical point for all molecular architectures designed for iSEF relates to the excitation energy of the triplet species and, in general, this parameter has not been well established by experiment. It is common practice to assume that SEF with pentacene derivatives is exoergic but the evidence for this assertion is weak. The triplet energy of TIPS-P was recently established[47] by PAC as being 7,940 ± 1,200 cm^{-1} but, as emphasized above, this value is not appropriate for PFP. There are two literature reports[26,40] that describe low-temperature phosphorescence from TIPS-P; the spectral profiles are remarkably similar and show a broad band with a maximum at 1,580 nm. We were unable to detect phosphorescence from crystals (Figure 5a) or solutions of TIPS-P[47] and we note that the inherent triplet yield for this compound is negligible in the absence of a spin-orbit accelerant.[30,47] Guldi *et al*.[26] also report low-temperature phosphorescence from a bis-pentacene derivative where the linkage is through the 6,6'-positions. Here, the phosphorescence peak lies at 1,620 nm, although the spectrum is quite broad making it difficult to assign the triplet energy. For this particular compound,[26] the central *meta*-phenylene spacer should limit electronic coupling between the terminals but even so the longest-lived triplet biexciton has a reported lifetime of only 2.6 ns in toluene at room temperature. The phosphorescence quantum yield, even at 77K, must be extremely low.

Because of the great significance of the triplet energy, we have sought to verify the phosphorescence spectra recorded for PFP. The spectra shown as Figure 5 are sharp and resolved into two peaks of similar intensity. That closely comparable spectra were obtained under disparate experimental conditions, and with different detectors, is reassuring. We have not been able to trace any convincing report of phosphorescence from pentacene or TIPS-P that might be compared with Figure 5. Of course, room-temperature phosphorescence from anthracene is very well known;[92] the spectral profile being similar to those shown in Figure 5 with the 0,0 transition located at 14,800 cm^{-1}.

There are several reports[92,93] of low-temperature phosphorescence from tetracene and diphenyltetracene. For example, weak phosphorescence has been described[93] for tetracene in MTHF at 77K with the emission peak lying at 10,900 ± 100 cm^{-1}. This represents a much lower triplet energy than is evident from earlier reports.[94,95]. The spectrum for tetracene is hampered by quite poor resolution[93] but exhibit fine structure similar to that found for PFP. Weak phosphorescence with a peak at 10,800 cm^{-1} has been reported[92] for tetracene dispersed in a thin film at room temperature. In this latter case, the detector was gated to avoid saturation from prompt fluorescence. Even so, the emission spectrum was dominated by delayed fluorescence such that the spectral profile for triplet emission, under these conditions, is unclear.[92] Phosphorescence from a single crystal of tetracene has its peak at 10,080 cm^{-1}.[96] Weak phosphorescence, also centered at 10,080 cm^{-1}, has been reported for TIPS-tetracene dispersed in a polystyrene matrix at room temperature.[97] This latter spectrum, recorded for dilute samples, appears to consist of two closely-spaced transitions but contamination from fluorescence prevents easy comparison with the spectra shown in Figure 5. As such, our phosphorescence spectra for PFP are not inconsistent with literature data for smaller polyacenes but further support would be useful.

Little information exists regarding the radiative lifetimes for the triplet states of the longer polyacenes but these are likely to exceed 10 s; the experimental value for naphthalene[98] at 77K is 63 s and this lifetime should increase with increasing size of the polyacene.[99,100] With a triplet lifetime of a few ns, the phosphorescence quantum yield would be $<10^{-9}$, making the emission very difficult to resolve from the baseline. A triplet lifetime of 10 μs would equate to an emission quantum yield of ca. 10^{-6}. This is in the range where the signal should be resolvable but quantitative measurements would be hazardous, especially in the near-IR region. It might be noted, however, that low yields of singlet molecular oxygen in water, where the lifetime is *ca.* 4 μs,[101] can be monitored easily with contemporary instrumentation.[102] The experimental measurement of room-temperature phosphorescence of certain polyacenes is hampered by the occurrence of delayed fluorescence and we have encountered this problem with PFP, despite the use of blocking filters.

The only realistic candidate for the phosphorescent state observed with PFP is the independent triplet pair and we have assigned the total triplet excitation energy content for this (relatively) long-lived species as being 14,580 cm^{-1}. This is less than the equivalent singlet excitation energy of 15,165 cm^{-1}. This means that iSEF is exoergic by almost 600 cm^{-1} while, at the same time, reverse population of S_G is not completely prohibited. We have no experimental means to establish excitation energies for the spin-correlated, triplet biexciton and our analysis assumes that there is zero energy change associated with this critical spin decorrelation step!

A point of possible contention concerns the introduction of a radiationless process that competes with spin decorrelation. This is made necessary by the need to explain enthalpy changes occurring on very fast and fast timescales and is an essential part of our analysis. There is experimental evidence for weak delayed fluorescence which is consistent with triplet-triplet an-

nihilation at the ^{1}[T_T] stage. This would lead to a certain degree of recycling between the two "singlet" states (Equation 9). The results, however, do not exclude separate internal conversion from ^{1}[T_T] to reform the ground state, although this step could not be responsible for the delayed fluorescence. The simplest mechanism that explains all the observations, therefore, has competition between spin decorrelation and TTA (Scheme 2). According to Equation 8, recycling is restricted to a few cycles but nonetheless it is an energy wastage step because of the partial restoration of the ground state at each cycle.[80] There is a very fine balance between obtaining a long-lived, independent triplet pair and ensuring quantitative spin decorrelation. The two objectives appear to be mutually exclusive.

Solvent polarity, but not temperature,[67] has an important influence on the photophysics for PFP and a polar environment increases the probability of triplet formation. Such behavior has been reported before for TIPS-P-based bichromophores where the linkage is *via* the 6,6'-ethynylene sites.[72,103] Interestingly, no such polarity effect was found with a set of directly-linked 2,2'-bichromophores.[27,28,104,105] In this latter case, it was proposed that vibronic coupling to intramolecular modes of the bichromophore facilitates strong mixing between the correlated triplet pair state and the local excitonic state, despite weak direct coupling. The net result is extremely fast iSEF. For PFP, increased solvent polarity leads to faster rates of both formation and decorrelation of the spin-correlated, triplet biexciton (Figure 7, Table 2). Since the competing internal conversion processes are unaffected by changes in solvent polarity, this represents a simple means for tuning the yield of the independent triplet pair. Indeed, the probability for iSEF increases to almost 100% in benzonitrile solution (Table 2). Conversely, the rate of spin decorrelation is very slow for PFP dispersed in a non-polar polymer film (i.e., Zeonex 480; see Supporting Information). Here, the lifetime of ^{1}[T_T] measured by transient absorption spectroscopy is extended to 300 ± 20 ns while that for the independent triplet pair is essentially unaffected and remains at 6.5 ± 1.2 μs. This increased stability of the spin-correlated, triplet biexciton is at the cost of a significantly reduced yield.

The solvent polarity effect is most likely a signature of intramolecular charge-transfer interactions between the terminal chromophores[27,28] This introduces an element of symmetry breaking[106] but there is no spectroscopic or kinetic evidence to implicate the intermediacy of a long-lived, charge-separated state. The importance of this type of charge-transfer mediation of iSEF will depend on the inherent rate of triplet formation for that particular molecular system. In the event that k_D is much faster than internal conversion, there will be no obvious effect of introducing charge-transfer character; this is the case with the directly-linked systems referenced above.[27,28,104,105] Where k_D is much slower than internal conversion, the advantage of incorporating charge-transfer effects are also unlikely to be substantial. It is with cases where the rate of iSEF is comparable to the rate of internal conversion that charge-transfer effects will be most noticeable. This is the situation with PFP.

We could identify only one example of a TIPS-P-based bichromophore where the lifetime of the independent triplet pair exceeds that recorded for PFP. The example in question has a fully-saturated bicyclooctane bridge connecting the 2,2'-positions and provides for a triplet lifetime of 18 μs in chloroform solution.[104] However, fluorescence quenching is minimal for this derivative and spin decorrelation occurs on the μs timescale such that the yield of the final triplet species must be low. The properties reported for PFP, therefore, especially in benzonitrile solution, appear to be superior to all other related TIPS-P-based bichromophores. This must be a consequence of the fluorene-based bridge which keeps the terminals isolated but in relatively close contact. The bridge, which is planar and unsaturated, couples well to the TIPS-P unit and does not allow structural heterogeneity.

The independent triplet pair for PFP is formed with an overall quantum yield of 0.44 in toluene at room temperature; this corresponds to an absolute triplet yield of 88%. Losses occur at each of the key stages due to competing radiationless processes (Scheme 2). About 40% of the initial excitation energy is lost because of fast internal conversion that competes with iSEF to form the spin-correlated, triplet pair. Spin decorrelation is relatively slow for PFP, taking a few hundreds of ns, and there is a further loss of about 40% due to competing triplet-triplet annihilation. The overall yield of the independent triplet pair is subject to kinetic control, which in turn is set by the electronic properties of the bridge. The PAC analysis has allowed recognition of a radiationless step competing with spin decorrelation but does not clarify the exact nature of this process. This step is difficult to quantify by transient absorption spectroscopy because spectral shifts are small and there are concerns about corresponding changes in the molar absorption coefficients.

Our analysis of this latter branching point has considered two limiting cases: namely, internal conversion to the ground state and triplet-triplet annihilation to give equal crops of S_G and G_G. The observation of delayed fluorescence, albeit weak, is clear indication that TTA occurs in this system but quantitative information is lacking. Conventional TTA is expected[9] to occur through the spin-correlated ^{1}[T_T] species, which is relatively long lived for PFP, and it is unlikely that internal conversion could occur from the ^{3}[T_T] intermediate (Scheme 1). However, the precise difference, if any, between ^{5}[T_T] and the independent triplet pair is rather indistinct. Little consideration has been given in the relevant literature regarding competition between spin decorrelation and radiationless decay. In most cases where the chromophores are strongly coupled, spin decorrelation is very fast and quantitative.[23] This suggests that the contribution of any competing processes is set by kinetics and there is no fundamental reason to consider internal conversion in cases where spin decorrelation is fast.

Temperature affects only the lifetime of the spin-correlated, triplet pair, which appears to follow Arrhenius behavior over a limited range in toluene. There is no such effect on the lifetimes of either the excited-singlet state or the independent triplet pair. Unfortunately, it is not feasible to assign this temperature dependence to any particular processes. We would expect an activation energy for intramolecular TTA, especially where the triplet excitation energy is somewhat less than one-half the corresponding singlet excitation energy, since this will involve through-bond electron exchange.[107] It is not possible, however, to isolate TTA from spin decorrelation and the crop of delayed fluorescence cannot be measured with sufficient precision for quantitative measurements.

CONCLUDING REMARKS

The main objective of this work was to engineer a molecular system capable of generating a long-lived, independent triplet pair in high yield via efficient iSEF under illumination with red light. The basic rationale was based on prior experimental work reported by many different research groups. The fluorene-based

spacer functions extremely well in this regard and provides spatial integrity, electronic isolation, improved solubility and good connection to the terminal chromophores; evidence for the latter is derived from cyclic voltammetry (Figure S26). The net result is the production of a triplet pair in 44% quantum yield having a lifetime of almost 10 μs in de-aerated toluene at room temperature. The yield is increased in a polar solvent, without shortening the triplet lifetime, and the iSEF course of action is maintained when the bichromophore is dispersed in a nonpolar film.

The generic process of iSEF presents interesting mechanistic challenges[23] and it is possible that there is a high degree of system dependence. Time-resolved optical spectroscopy provides the fundamental kinetic information and, subject to accurate knowledge of differential molar absorption coefficients, can be used to establish net reaction yields. Additional spectroscopic tools are needed, however, to delve deeper into the reaction mechanism. Both vibrational spectroscopy[43] and time-resolved EPR spectroscopy[75-77] have provided new insight into aspects of the iSEF process. Here, we report the first application of photoacoustic calorimetry (PAC) to better understand the energy balance underpinning iSEF. In essence, PAC provides information about enthalpy changes that accompany photophysical events. The temporal resolution is set by the type of transducer and the excitation pulse. The instrument used to monitor heat release for PFP in solution nicely accommodates three temporal regimes that combine to define the overall transformation of S_G to $[T\_T]^{IND}$. In particular, the time window of the 2.25 MHz transducer isolates the spin decorrelation process, which is the most elusive step in the overall process. Regardless of the finer details, PAC demonstrates that the probability for formation of the independent triplet pair is linked to competing radiationless decay of the triplet biexciton. The capability to quantify the heat released during this step is paramount to establishing the mechanism.

ASSOCIATED CONTENT

Supporting Information. Includes details for the synthesis and characterization of PFP, temperature effects, cyclic voltammogram, and further spectroscopic information. This material is available free of charge via the Internet at http://pubs.acs.org.

AUTHOR INFORMATION

Corresponding Author

*Prof Anthony Harriman: anthony.harriman@ncl.ac.uk.

Author ORCID numbers

JKGK: 0000-0001-7281-1257

AA: 0000-0001-8904-9377

AH: 0000-0003-0679-2232

NVT: 0000-0002-8504-2335

ADW: 0000-0001-6946-2391

FAS: 0000-0002-9339-7259

CS: 0000-0001-7004-0110

LGA: 0000-0002-3223-4819

Present Address

†Present Address: Department of Polymer Engineering, Faculty of Technology, Duzce University, 81620 Duzce, Turkey.

Author Contributions

All authors have given approval to the final version of the manuscript. The authors declare no conflicts of interest.

ACKNOWLEDGMENT

We thank Newcastle University, Tampere University and Coimbra University for providing access to key facilities to undertake this research project. We also thank STFC CLF Octopus Facility for PoC access to the NIR emission microscope. We acknowledge financial support from the Portuguese Science Foundation (UIDB/QUI/00313/2020, Roteiro/ 0152/2013/022124) and from the European Union's Horizon 2020 Research and Innovation Programme under grant agreement no. 654148 Laser Lab-Europe. AA thanks TUBITAK (The Scientific and Technological Research Council of Turkey) for the award of a research fellowship.

ABBREVIATIONS

TLC, thin layer chromatography. PAC, photoacoustic calorimetry. EPR, electron paramagnetic resonance. MTHF, 2-methyltetrahydrofuran.

REFERENCES

(1) Singh, S.; Jones, W. J.; Siebrand, W.; Stoicheff, B. P.; Schneider, W. G. Laser Generation of Excitons and Fluorescence in Anthracene Crystals. *J. Chem. Phys.* **1965**, *42*, 330-342.

(2) Swenberg, C. E.; Stacy, W. T. Bimolecular Radiationless Transitions in Crystalline Tetracene. *Chem. Phys. Lett.* **1968**, *2*, 327-328.

(3) Geacintov, N.; Pope, M.; Vogel, F. E., III. Effect of Magnetic Field on the Fluorescence of Tetracene Crystals: Exciton Fission. *Phys. Rev. Lett.* **1969**, *22*, 593-596.

(4) Greyson, E. C.; Stepp, B. R.; Chen, X. D.; Schwerin, A. F.; Paci, I.; Smith, M. B.; Akdag, A.; Johnson, J. C.; Nozik, A. J.; Michl, J.; Ratner, M. A. Singlet Exciton Fission for Solar Cell Applications. Energy Aspects of Interchromophore Coupling. *J. Phys. Chem. B* **2010**, *114*, 14223-14232.

(5) Miyata, K.; Conrad-Burton, F. S.; Geyer, F. L.; Zhu, X.-Y. Triplet Pair States in Singlet Fission. *Chem. Rev.* **2019**, *119*, 4261-4292.

(6) Khan, S.; Mazumdar, S. Theory of Transient Excited State Absorptions in Pentacene and Derivatives: Triplet−Triplet Biexciton Versus Free Triplets. *J. Phys. Chem. Lett.* **2017**, *8*, 5943-5948.

(7) Pinheiro, M.; Machado, F. B. C.; Plasser, F.; Aquino, A. J. A.; Lischka, H. A Systematic Analysis of Excitonic Properties to Seek Optimal Singlet Fission: The BN-Substitution Patterns in Tetracene. *J. Mater. Chem. C* **2020**, *8*, 7793-7804.

(8) Buchanan, E. A.; Havlas, Z.; Michl, J. Singlet Fission: Optimization of Chromophore Dimer Geometry. *Adv. Quantum Chem.* **2017**, *75*, 175-227.

(9) Sternlicht, H.; Nieman, G. C.; Robinson, G. W. Triplet-Triplet Annihilation and Delayed Fluorescence in Molecular Aggregates. *J. Chem. Phys*. **1963**, *38*, 1326.

(10) Dilbeck, T.; Hanson, K. Molecular Photon Upconversion Solar Cells Using Multilayer Assemblies: Progress and Prospects. *J Phys Chem Lett*. **2018**, *9*, 5810-5821.

(11) Trupke, T.; Green, M. A.; Würfel, P. Improving Solar Cell Efficiencies by Up-Conversion of Sub-Band-Gap Light, *J. Appl. Phys.* **2002**, *92*, 4117-4122.

(12) Smith, M. B.; Michl, J. Singlet Fission. *Chem. Rev*. **2010**, *110*, 6891-6936.

(13) Smith, M. B.; Michl, J. Recent Advances in Singlet Fission. *Ann. Rev. Phys. Chem*. **2013**, *64*, 361-386.

(14) Grieco, C.; Kennehan, E. R.; Kim, H.; Pensack, R. D.; Brigeman, A. N.; Rimshaw, A.; Payne, M. M.; Anthony, J. E.; Giebink, N. C.; Scholes, G. D.; Asbury, J. B. Direct Observation of Correlated Triplet Pair Dynamics during Singlet Fission Using Ultrafast Mid-IR Spectroscopy. *J. Phys. Chem. C* **2018**, *122*, 2012-2022.

(15) Folie, B. D.; Haber, J. B.; Refaely-Abramson, S.; Neaton, J. B.; Ginsberg, N. S. Long-Lived Correlated Triplet Pairs in a π‑Stacked Crystalline Pentacene Derivative. *J. Am. Chem. Soc.* **2018**, *140*, 2326-2335.

(16) Grieco, C.; Doucette, G. S.; Pensack, R. D.; Payne, M. M.; Rimshaw, A.; Scholes, G. D.; Anthony, J. E.; Asbury, J. B. Dynamic Exchange During Triplet Transport in Nanocrystalline TIPS-Pentacene Films. *J. Am. Chem. Soc*. **2016**, *138*, 16069-16080.

(17) Ramanan, C.; Smeigh, A. L.; Anthony, J. E.; Marks, T. J.; Wasielewski, M. R. Competition between Singlet Fission and Charge Separation in Solution-Processed Blend Films of 6,13-Bis(triisopropylsilylethynyl)-Pentacene with Sterically-Encumbered Perylene-3,4:9,10-bis(dicarboximide)s. *J. Am. Chem. Soc*. **2012**, *134*, 386-397.

(18) Monahan, N.; Zhu X.-Y. Charge Transfer–Mediated Singlet Fission. *Ann. Rev. Phys. Chem*. **2015**, *66*, 601-618.

(19) Grieco, C.; Doucette, G. S.; Munson, K. T.; Swartzfager, J. R.; Munro, J. M.; Anthony, J. E.; Dabo, I.; Asbury, J. B. Vibrational Probe of the Origin of Singlet Exciton Fission in TIPS-Pentacene Solutions. *J. Chem. Phys*. **2019**, *151*, 154701.

(20) Wu, Y.; Liu, K.; Liu, H.; Zhang, Y.; Zhang, H.; Yao, J.; Fu, H. Impact of Intermolecular Distance on Singlet Fission in a Series of TIPS Pentacene Compounds. *J. Phys. Chem. Lett*. **2014**, *5*, 3451-3455.

(21) Lubert-Perquel, D.; Salvadori, E.; Dyson, M.; Stavrinou, P. N.; Montis, R.; Nagashima, H.; Kobori, Y.; Heutz, S.; Kay, C. W. M. Identifying Triplet Pathways in Dilute Pentacene Films. *Nature Commun*. **2018**, *9*, 4222.

(22) Wong, C. Y.; Penwell, S. B.; Cotts, B. L.; Noriega, R.; Wu, H.; Ginsberg, N. S. Revealing Exciton Dynamics in a Small-Molecule Organic Semiconducting Film with Subdomain Transient Absorption Microscopy. *J. Phys. Chem. C* **2013**, *117*, 22111-22122.

(23) Korovina, N.; Pompetti, N.; Johnson, J. C. Lessons from Intramolecular Singlet Fission with Covalently Bound Chromophores. *J. Chem. Phys*. **2020**, *152*, 040904.

(24) Johnson, J. C.; Akdag, A.; Zamadar, M.; Chen, X.; Schwerin, A. F.; Paci, I.; Smith, M. B.; Havlas, Z.; Miller, J. R.; Ratner, M. A.; Nozik, A. R.; Michl, J. Toward Designed Singlet Fission: Solution Photophysics of Two Indirectly Coupled Covalent Dimers of 1,3-Diphenylisobenzofuran. *J. Phys. Chem. B* **2013**, *117*, 4680-4695.

(25) Johnson, J. C.; Nozik, A. J.; Michl, J. High Triplet Yield from Singlet Fission in a Thin Film of 1,3-Diphenylisobenzofuran. *J. Am. Chem. Soc*. **2010**, *132*, 16302-16303.

(26) Zirzlmeier, J.; Lehnherr, D.; Coto, P. B.; Chernick, E. T.; Casillas, R.; Basel, B. S.; Thoss, M.; Tykwinski, R. R.; Guldi, D. M. Singlet Fission in Pentacene Dimers. *Proc. Natl. Acad. Sci. USA* **2015**, *112*, 5325-5330.

(27) Sanders, S. N.; Kumarasamy, E.; Pun, A. B.; Appavoo, K.; Steigerwald, M. L.; Campos, L. M.; Sfeir, M. Y. Exciton Correlations in Intramolecular Singlet Fission. *J. Am. Chem. Soc.* **2016**, *138*, 7289-7297.

(28) Sanders, S. N.; Kumarasamy, E.; Pun, A. B.; Steigerwald, M. L.; Sfeir, M. Y.; Campos, L. M. Singlet Fission in Polypentacene. *Chem*. **2016**, *1*, 505-511.

(29) Sakuma, T.; Sakai, H.; Araki, Y.; Mori, T.; Wada, T.; Tkachenko, N. V.; Hasobe, T. Long-Lived Triplet Excited States of Bent-Shaped Pentacene Dimers by Intramolecular Singlet Fission. *J. Phys. Chem. A* **2016**, *120*, 1867-1875.

(30) Alagna, N.; Lustres, J. L. P. ; Wollscheid, N.; Luo, Q.-Q.; Han, J.; Dreuw, A.; Geyer, F. L.; Brosius, V.; Bunz, U. H. F.; Buckup, T. Singlet Fission in Tetraaza-TIPS-Pentacene Oligomers: From fs Excitation to μs Triplet Decay via the Biexcitonic State. *J. Phys. Chem. B* **2019**, *123*, 10780-10793.

(31) Casillas, R.; Adam, M.; Coto, P. B.; Waterloo, A. R.; Zirzlmeier, J.; Reddy, S. R.; Hampel, F.; McDonald, R.; Tykwinski, R. R.; Thoss, M.; Guldi, D. M. Intermolecular Singlet Fission in Unsymmetrical Derivatives of Pentacene in Solution. *Adv. Ener. Mater*. **2019**, *9*, 1802221.

(32) Busby, E.; Berkelbach, T. C.; Kumar, B.; Chernikov, A.; Zhong, Y.; Hlaing, H.; Zhu, X.-Y.: Heinz, A. F.; Hybertsen, M. S.; Sfeir, M. Y.; Reichman, D. R.; Nuckolls, C.; Yaffe, O. Multiphonon Relaxation Slows Singlet Fission in Crystalline Hexacene. *J. Am. Chem. Soc*. **2014**, *136*, 10654-10660.

(33) Thampi, A.; Stern, H. L.; Cheminal, A.; Tayebjee, M. J. Y.; Petty, II, A. J.; Anthony, J. E.; Rao, A. Elucidation of Excitation Energy Dependent Correlated Triplet Pair Formation Pathways in an Endothermic Singlet Fission System. *J. Am. Chem. Soc*. **2018**, *140*, 4613-4622.

(34) Greyson, E. C.; Vura-Weis, J.; Michl, J.; Ratner, M. A. Maximizing Singlet Fission in Organic Dimers. Theoretical Investigation of Triplet Yield in the Regime of Localized Excitation and Fast Coherent Electron Transfer. *J. Phys. Chem. B* **2010**, *114*, 14168-14177.

(35) Sakai, H.; Inaya, R.; Nagashima, H.; Nakamura, S.;Kobori, Y.; Tkachenko, N. V.; Hasobe, T. Multiexciton Dynamics Depending on Intramolecular Orientations in Pentacene Dimers: Recombination and Dissociation of Correlated Triplet Pairs. *J. Phys. Chem. Lett*. **2018**, *9*, 3354-3360.

(36) Johnson, J. C.; Nozik, A. J.; Michl, J. The Role of Chromophore Coupling in Singlet Fission. *Acc. Chem. Res*. **2013**, *46*, 1290-1299.

(37) Karlsson, J. K. G.; Atahan, A.; Harriman, A.; Tojo, S.; Fujitsuka, M.; Majima, T. Pulse Radiolysis of TIPS-Pentacene and a Fluorene-Bridged Bis(pentacene): Evidence for Intramolecular Singlet-Exciton Fission. *J. Phys. Chem. Lett.* **2018**, *9*, 3934-3938.

(38) Dover, C. B.; Gallaher, J. K.; Frazer, L.; Tapping, P. C.; Petty, A. J.; Crossley, M. J.; Anthony, J. E.; Kee, T. W.; Schmidt, T. W. Endothermic Singlet Fission is Hindered by Excimer Formation. *Nature Chem*. **2018**, *10*, 305-310.

(39) Busby, E.; Xia, J.; Wu, Q.; Low, J. Z.; Song, R.; Miller, J. R.; Zhu, X. Y.; Campos, L. M.; Sfeir, M. Y. A Design Strategy for Intramolecular Singlet Fission Mediated by Charge-Transfer States in Donor-Acceptor Organic Materials. *Nature Mater*. **2015**, *14*, 426-433.

(40) Zhang, Y.-D.; Wu, Y.; Xu, Y.; Wang, Q.; Liu, K.; Chen, J.-W.; Cao, J.-J.; Zhang, C.; Fu, H.; Zhang, H.-L. Excessive Exoergicity Reduces Singlet Exciton Fission Efficiency of Heteroacenes in Solutions. *J. Am. Chem. Soc*. **2016**, *138*, 6739-6745.

(41) Pace, N. A.; Rugg, B. K.; Chang, C. H.; Reid, O. G.; Thorley, K. J.; Parkin, S.; Anthony, J. E.; Johnson, J. C. Conversion Between Triplet Pair States is Controlled by Molecular Coupling in Pentadithiophene Thin Films. *Chem. Sci*. **2020**, *11*, 7226-7238.

(42) Gish, M. K.: Pace, N. A.; Rumbles, G.; Johnson, J. C. Emerging Design Principles for Enhanced Solar Energy Utilization with Singlet Fission. *J. Phys. Chem. C*. **2019**, *123*, 3923-3934.

(43) Chen, M.; Krzyaniak, M. D.; Nelson, J. N.; Bae, Y. J.; Harvey, S. M.; Schaller, R. D.; Young, R. M.; Wasielewski, M. R. Quintet-Triplet Mixing Determines the Fate of the Multiexciton State Produced by Singlet Fission in a Terrylenediimide Dimer at Room Temperature. *Proc. Natl. Acad. Sci. U. S. A*. **2019**, *116*, 8178-8183.

(44) Berkelbach, T. C.; Hybertsen, M. S.; Reichman, D. R. Microscopic Theory of Singlet Exciton Fission. II. Application to Pentacene Dimers and the Role of Superexchange. *J. Chem. Phys.* **2013**, *138*, 114103.

(45) Maliakal, A.; Raghavachari, K.; Katz, H.; Chandross, E.; Siegrist, T. Photochemical Stability of Pentacene and a Substituted Pentacene in Solution and in Thin Films. *Chem. Mater.* **2004**, *16*, 4980-4986.

(46) Anthony, J. E.; Brooks, J. S.; Eaton, D. L.; Parkin, S. R. Functionalized Pentacene: Improved Electronic Properties from Control of Solid-State Order. *J. Am. Chem. Soc.* **2001**, *123*, 9482-9483.

(47) Schaberle, F. A.; Serpa, C.; Arnaut, L. G.; Ward, A. D.; Karlsson, J. K. G.; Atahan, A.; Harriman, A. The Photophysical Properties of Triisopropylsilyl-ethynylpentacene-A Molecule with an Unusually Large Singlet-Triplet Energy Gap-In Solution and Solid Phases. *Chem.* **2020**, *2*, 545-564.

(48) Pun, A. B.; Asadpoordarvish, A.; Kumarasamy, E.; Tayebjee, M. J. Y.; Niesner, D.; McCamey, D. R.; Sanders, S. N.; Campos, L. M.; Sfeir, M. Y. Ultra-Fast Intramolecular Singlet Fission to Persistent Multiexcitons by Molecular Design, *Nat. Chem.* **2019**, *11*, 821-828.

(49) Gilligan, A. T.; Miller, E. G.; Sammakia, T.; Damrauer, N. H. Using Structurally Well-Defined Norbornyl-Bridged Acene Dimers to Map a Mechanistic Landscape for Correlated Triplet Formation in Singlet Fission. *J. Am. Chem. Soc*. **2019**, *141*, 5961-5971.

(50) Hetzer, C.; Guldi, D. M.; Tykwinski, R. R. Pentacene Dimers as a Critical Tool for the Investigation of Intramolecular Singlet Fission. *Chem. Eur. J*. **2018**, *24*, 8425-8457.

(51) Basel, B. S.; Papadopoulos, J.; Thiel, D.; Casillas, R.; Zirlmeier, J.; Clark, T.; Guldi, D. M.; Tykwinski, R. R. Pentacenes: A Molecular Ruler for Singlet Fission, *Trends Chem*. **2019**, *1*, 11-21.

(52) Arnaut, L. G.; Caldwell, R. A.; Elbert, J. E.; Melton, L. A. Recent Advances in Photoacoustic Calorimetry – Theoretical Basis and

Improvements in Experimental Design. *Rev. Sci. Instrum*. **1992**, *63*, 5381-5389.

(53) Schaberle, F. A. N.; Numes, R. M. D.; Barroso, M.; Serpa, C.; Arnaut, L. G. Analytical Solution for Time-Resolved Photoacoustic Calorimetry Data and Applications to Two Typical Photoreactions. *Photochem. Photobiol. Sci*. **2010**, *9*, 812-822.

(54) Braslavsky, S. E.; Heibel, G. E. Time-Resolved Photothermal and Photoacoustic Methods Applied to Photoinduced Processes in Solution. *Chem. Rev*. **1992**, *92*, 1381-1410.

(55) Pineiro, M.; Carvalho, A. L.; Pereira, M. M.; Gonsalves, A. M. D. R.; Arnaut, L. G.; Formosinho, S. Photoacoustic Measurements of Porphyrin Triplet-State Quantum Yields and Singlet-Oxygen Efficiencies. *Chem. Eur. J*. **1998**, *4*, 2299-2307.

(56) Schaberle, F. A.; Rego Filho, F. A. M. G.; Reis, L. A.; Arnaut, L. G. Assessment of Lifetime Resolution Limits in Time-Resolved Photoacoustic Calorimetry vs. Transducer Frequencies: Setting the Stage for Picosecond Resolution. *Photochem. Photobiol. Sci*. **2016**, *15*, 204-210.

(57) Seybold, P. G.; Gouterman, M. Porphyrins XIII: Fluorescence Spectra and Quantum Yields. *J. Mol. Spectrosc*. **1969**, *31*, 1-13.

(58) Pelado, B.; Abou-Chahine, F.; Calbo, J.; Caballero, R.; de la Cruz, P.; Junquera-Hernandez, J. M.; Ortí, E.; Tkachenko, N. V.; Langa, F. Role of the Bridge in Photoinduced Electron Transfer in Porphyrin-Fullerene Dyads. *Chem. Eur. J*. **2015**, *21*, 5814-5825.

(59) Berera, R.; van Grondelle, R.; Kennis, J. T. M. Ultrafast Transient Absorption Spectroscopy: Principles and Application to Photosynthetic Systems. *Photosynth. Res*. **2009**, *101*, 105-118.

(60) Van Stokkum, I. H. M.; Larsen, D. S.; Van Grondelle, R. Global and Target Analysis of Time-Resolved Spectra. *Biochim. Biophys. Acta* **2004**, *1657*, 82–104.

(61) Pineiro, M.; Gonsalves, A. M. D. R.; Pereira, M. M.; Formosinho, S. J.; Arnaut, L. G. New Halogenated Phenylbacteriochlorins and Their Efficiency in Singlet-Oxygen Sensitization *J. Phys. Chem. A* **2002**, *106*, 3787-3795.

(62) Gomes, P. J. S.; Serpa, C.; Arnaut, L. G. About Biphenyl First Excited Triplet State Energy. *J. Photochem. Photobiol. A: Chem.* **2006**, *184*, 228-233.

(63) de Melo, J. S. S.; Burrows, H. D.; Serpa, C.; Arnaut, L. G. The Triplet State of Indigo. *Angew. Chem. Int. Ed*. **2007**, *46*, 2094-2096.

(64) Gallimore, P. J.; Davidson, N. M.; Kalberer, M.; Pope, F. D.; Ward, A. D. 1064 nm Dispersive Raman Microspectroscopy and Optical Trapping of Pharmaceutical Aerosols. *Anal. Chem*. **2018**, *90*, 8838-8844.

(65) Yeow, E. K. L.; Braslavsky, S. E. Quenching of Zinc Tetraphenylporphine by Oxygen and by 1,4-Benzoquinone in Nitrile Solvents: An Optoacoustic Spectroscopy Study. *Phys. Chem. Chem. Phys*. **2002**, *4*, 239-247.

(66) Engler, B. P.; Harrah, L. A. Viscosity and Density of 2-Methyltetrahydrofuran as a Function of Temperature. National Technical Reports Library, 1979, NTIS Issue Number 197917.

(67) Wilson, M. W. B.; Rao, A.; Johnson, K.; Gélinas, S.; di Pietro, R.; Clark, J.; Friend, R. H. Temperature-Independent Singlet Exciton Fission in Tetracene**.** *J. Am. Chem. Soc.* **2013**, *135*, 16680–16688.

(68) Ruckebusch, C.; Sliwa, M.; Pernot, P.; de Juan, A.; Tauler, R. Comprehensive Data Analysis of Femtosecond Transient Absorption Spectra: A Review. *J. Photochem. Photobiol. C: Photochem. Rev*. **2012**, *13*, 1-27.

(69) Grellmann, K. H.; Scholz, G. Determination of Decay Constants with a Sampling Flash Apparatus. The Triplet State Lifetimes of Anthracene and Pyrene in Fluid Solutions. *Chem. Phys. Lett*. **1979**, *62*, 64-71.

(70) Imperiale, C. J.; Green, P. B.; Miller, E. G.; Damrauer, N. H.; Wilson, M. W. B. Triplet-Fusion Upconversion Using a Rigid Tetracene Homodimer. *J. Phys. Chem. Lett.* **2019**, *10*, 7463–7469.

(71) Zimmerman, P. M.; Bell, F.; Casanova, D.; Head-Gordon, M. Mechanism for Singlet Fission in Pentacene and Tetracene: From Single Exciton to Two Triplets. *J. Am. Chem. Soc*. **2011**, *133*, 19944-19952.

(72) Lukman, S.; Musser, A. J.; Chen, K.; Athanasopoulos, S.; Yong, C. K.; Zeng, Z.; Ye, Q.; Chi, C.; Hodgkiss, J. M.; Wu, J.; et al. Tuneable Singlet Exciton Fission and Triplet−Triplet Annihilation in an Orthogonal Pentacene Dimer. *Adv. Funct. Mater*. **2015**, *25*, 5452-5461.

(73) Lee, T. S.; Lin, Y.-H. L.; Kim, H.; Pensack, R. D.; Rand, B. P.; Scholes**,** G. D. Triplet Energy Transfer Governs the Dissociation of the Correlated Triplet Pair in Exothermic Singlet Fission. *J. Phys. Chem. Lett.* **2018**, *9*, 4087-4095.

(74) Niu, M.-S.; Yang, X.-Y.; Qin, C.-C.; Bi, P.-Q.; Lyu, C.-K.; Feng, L.; Qin, W.; Gao, K.; Ha, X.-T. Competition between Singlet Fission and Singlet Exciton Dissociation at the Interface in TIPS-Pentacene:IT-4F Blend. *Org. Electronics* **2019**, *71*, 296-302.

(75) Nagashima, H.; Kawaoka, S.; Matsui, Y.; Tachikawa, T.; Ikeda, H.; Kobori, Y. Time-Resolved EPR Study on Singlet-Fission Induced Quintet Generation and Subsequent Triplet Dissociation in TIPS-Phenyl-Tetracene Aggregates. *J. Photopolym. Sci. Technol*. **2018**, *31*, 163-167.

(76) Biskup, T. Structure–Function Relationship of Organic Semiconductors: Detailed Insights from Time-Resolved EPR Spectroscopy. *Front. Chem*. **2019**, *7*, 10.

(77) Bayliss, S. L.; Kraffert, F.; Wang, R.; Zhang, C.-F.; Bittl, R.; Behrends, J. Tuning Spin Dynamics in Crystalline Tetracene. *J. Phys. Chem. Lett.* **2019**, *10*, 1908-1913.

(78) Pensack, R. D.; Ostroumov, E. E.; Tilley, A. J.; Mazza, S.; Grieco, C.; Thorley, K. J.; Asbury, J. B.; Seferos, D. S.; Anthony, J. E.; Scholes, G. D. Observation of Two Triplet-Pair Intermediates in Singlet Exciton Fission. *J. Phys. Chem. Lett*. **2016**, *7*, 2370-2375.

(79) Al-Aqar, R.; Benniston, A. C.; Harriman, A.; Perks, T. Structural Dynamics and Barrier Crossing Observed for a Fluorescent O-Doped Polycyclic Aromatic Hydrocarbon. *ChemPhotoChem* **2017**, *1*, 198-205.

(80) Baleizao, C.; Berberan-Santos, M. N. Thermally Activated Delayed Fluorescence as a Cycling Process between Excited Singlet and Triplet States: Application to the Fullerenes. *J. Chem. Phys*. **2007**, *126*, 204510.

(81) Dias, F. B.; Bourdakos, K. N.; Jankus, V.; Moss, K. C.; Kamtekar, K. T.; Bhalla, V.; Santos, J.; Bryce, M. R.; Monkman, A. P. Triplet Harvesting with 100% Efficiency by Way of Thermally Activated Delayed Fluorescence in Charge Transfer OLED Emitters. *Adv. Mater*. **2013**, *25*, 3707-3714.

(82) Stachelek, P.; Alsimaree, A. A,; Alnoman, R. B.; Harriman, A,; Knight, J. G. Thermally-Activated, Delayed Fluorescence in O,B,O- and N,B,O-Strapped Boron Dipyrromethene Derivatives. *J. Phys. Chem. A* **2017**, *121*, 2096-2107.

(83) Wallikewitz, B. H.; Kabra, D.; Gelinas, S.; Friend, R. H. Triplet Dynamics in Fluorescent Polymer Light-Emitting Diodes. *Phys. Rev. B* **2012**, 85, 045209.

(84) Ito, S.; Nagami, T.; Nakano, M. Molecular Design for Efficient Singlet Fission. *J. Photochem. Photobiol. C: Photochem. Rev*. **2018**, *34*, 85-120.

(85) Margulies, E. A.; Logsdon, J. L.; Miller, C. E.; Ma, L.; Simonoff, E.; Young, R. M.; Schatz, G. C.; Wasielewski, M. R. Direct Observation of a Charge-Transfer State Preceding High-Yield Singlet Fission in Terrylenediimide Thin Films. *J. Am. Chem. Soc*. **2017**, *139*, 663-671.

(86) Borkent, J. H.; Verhoeven, J. W.; de Boer, T. Charge-Transfer Fluorescence from Electron Donor-Acceptor Cyclophanes; Influence of Geometry and Solvent Polarity. *Chem. Phys. Lett*. **1976**, *42*, 50-55.

(87) Heitele, H.; Finckh, P.; Weeren, S.; Pöllinger, F.; Michel-Beyerle, M. E. Solvent Polarity Effects on Intramolecular Electron Transfer. 1. Energetic Aspects. *J. Phys. Chem.* **1989**, *93*, 5173-5179.

(88) Beljonne, D.; Yamagata, H.; Bredas, J. L.; Spano, F. C.; Olivier, Y. Charge-Transfer Excitations Steer the Davydov Splitting and Mediate Singlet Exciton Fission in Pentacene. *Phys. Rev. Lett.* **2013**, *110*, 226402.

(89) Heitele H.; Weeren S.; Pöllinger F.; Michel-Beyerle M. E. Solvent Polarity Effects on Thermodynamics and Kinetics of Intramolecular Electron Transfer Reactions. In: Jortner J., Pullman B. (eds) Perspectives in Photosynthesis. The Jerusalem Symposia on Quantum Chemistry and Biochemistry, 1990, Vol 22. Springer, Dordrecht.

(90) Dron, P. I.; Michl, J.; Johnson, J. C. Singlet Fission and Excimer Formation in Disordered Solids of Alkyl-Substituted 1,3-Diphenylisobenzofurans. *J. Phys. Chem. A* **2017**, *121*, 8596-8603.

(91) Miller, C. E.; Wasielewski, M. R.; Schatz, G. C. Modeling Singlet Fission in Rylene and Diketopyrrolopyrrole Derivatives: The Role of the Charge Transfer State in Superexchange and Excimer Formation. *J. Phys. Chem. C* **2017**, *121*, 10345-10350

(92) Reineke, S.; Baldo, M. A. Room Temperature Triplet State Spectroscopy of Organic Semiconductors. *Sci. Rep.* **2014**, *4*, 3797.

(93) Völcker, A.; Adick, H.-J.; Schmidt, R.; Brauer, H.-D. Near Infrared Phosphorescence Emission of Compounds with Low-Lying Triplet States. *Chem. Phys. Lett.* **1989**, *159*, 103-108.

(94) Lamola, A. A.; Herkstroeter, W. G.; Dalton, C.; Hammond, G. S. Excitation Energies of Azulene and Naphthacene Triplets. *J. Chem. Phys.* **1965**, *42*, 1715-1717.

(95) McGlynn, S. P.; Padhye, M. R.; Kasha, M. Lowest Triplet Levels of the Polyacenes. *J. Chem. Phys*. **1955**, *23*, 593-594.

(96) Tomkiewicz, Y.; Groff, R. P.; Avakian, P. Spectroscopic Approach to Energetics of Exciton Fission and Fusion in Tetracene Crystals. *J. Chem. Phys*. **1971**, *54*, 4504-4507.

(97) Stern, H. L.; Musser, A. J.; Gelinas, S.; Parkinson, P.; Herz, L. M,; Bruzek, M. J.; Anthony, J. E.; Friend, R. H.; Walker, B. J. Identification of a Triplet Pair Intermediate in Singlet Exciton Fission in Solution. *Proc. Natl. Acad. Sci. USA* **2015**, *112*, 7656-7661.

(98) Pedash, Y. F.; Prezhdo, O. V.; Kotelevskiy, S. I.; Prezhdo, V. V. Spin-Orbit Coupling and Luminescence Characteristics of Conjugated Organic Molecules. I. Polyacenes. *J. Mol. Struct. (TheoChem)* **2002**, *585*, 49-59.

(100) Nijegorodov, N.; Ramachandran, V.; Winkoun, D. P. The Dependence of the Absorption and Fluorescence Parameters, the Intersystem Crossing and Internal Conversion Rate Constants on the Number of Rings in Polyacene Molecules. *Spectrochim. Acta Part A: Mol. Biomol. Spectrosc.* **1997**, *53*, 1813-1824.

(101) Niedre, M.; Patterson, M. S.; Wilson, B. C. Direct Near-Infrared Luminescence Detection of Singlet Oxygen Generated by Photodynamic Therapy in Cells in vitro and Tissues in vivo. *Photochem. Photobiol.* **2002**, *75*, 382-391.

(102) Boso, G.; Ke, D.; Korzh, B.; Bouilloux, J.; Lange, N.; Zbinden, H. Time-Resolved Singlet-Oxygen Luminescence Detection with an Efficient and Practical Semiconductor Single-Photon Detector. *Biomed. Optics Exp.* **2016**, *7*, 211-224.

(103) Lukman, S.; Chen, K.; Hodgkiss, J. M.; Turban, D. H. P.; Hine, N. D. M.; Dong, S.; Wu, J.; Greenham, N. C.; Musser, A. J. Tuning the Role of Charge-Transfer States in Intramolecular Singlet Exciton Fission through Side-Group Engineering. *Nature Commun*. **2016**, ***7***, 13622.

(104) Kumarasamy, E.; Sanders, S. N.; Tayebjee, M. J. Y.; Asadpoordarvish, A.; Hele, T. J. H.; Fuemmeler, E. G.; Pun, A. B.; Yablon, L. M.; Low, J. Z.; Paley, D. W. et al., Tuning Singlet Fission in π-Bridge-π-Chromophores. *J. Am. Chem. Soc*. **2017**, *139*, 12488-12494.

(105) Fuemmeler, E. G.; Sanders, S. N.; Pun, A. B.; Kumarasamy, E.; Zeng, T.; Miyata, K.; Steigerwald, M. L.; Zhu, X.-Y.; Sfeir, M. Y.; Campos, L. M.; Ananth, N. A Direct Mechanism of Ultrafast Intramolecular Singlet Fission in Pentacene Dimers. *ACS Cent. Sci*. **2016**, *2*, 316‑324.

(106) Miyata, K.; Kurashige, Y.; Watanabe, K.; Sugimoto, T.; Takahashi, S.; Tanaka, S.; Takeya, J.; Yanai, T.; Matsumoto, Y. Coherent Singlet Fission Activated by Symmetry Breaking. *Nature Chem*. **2017**, *9*, 983-989.

(107) Ye, C.-Q.; Zhou, L. W.; Wang, X.-M.; Liang, Z.-Q. Photon Upconversion: from Two-Photon Absorption (TPA) to Triplet-Triplet Annihilation (TTA). *Phys. Chem. Chem. Phys*. **2016**, *18*, 10818-10835.

Insert Table of Contents artwork here